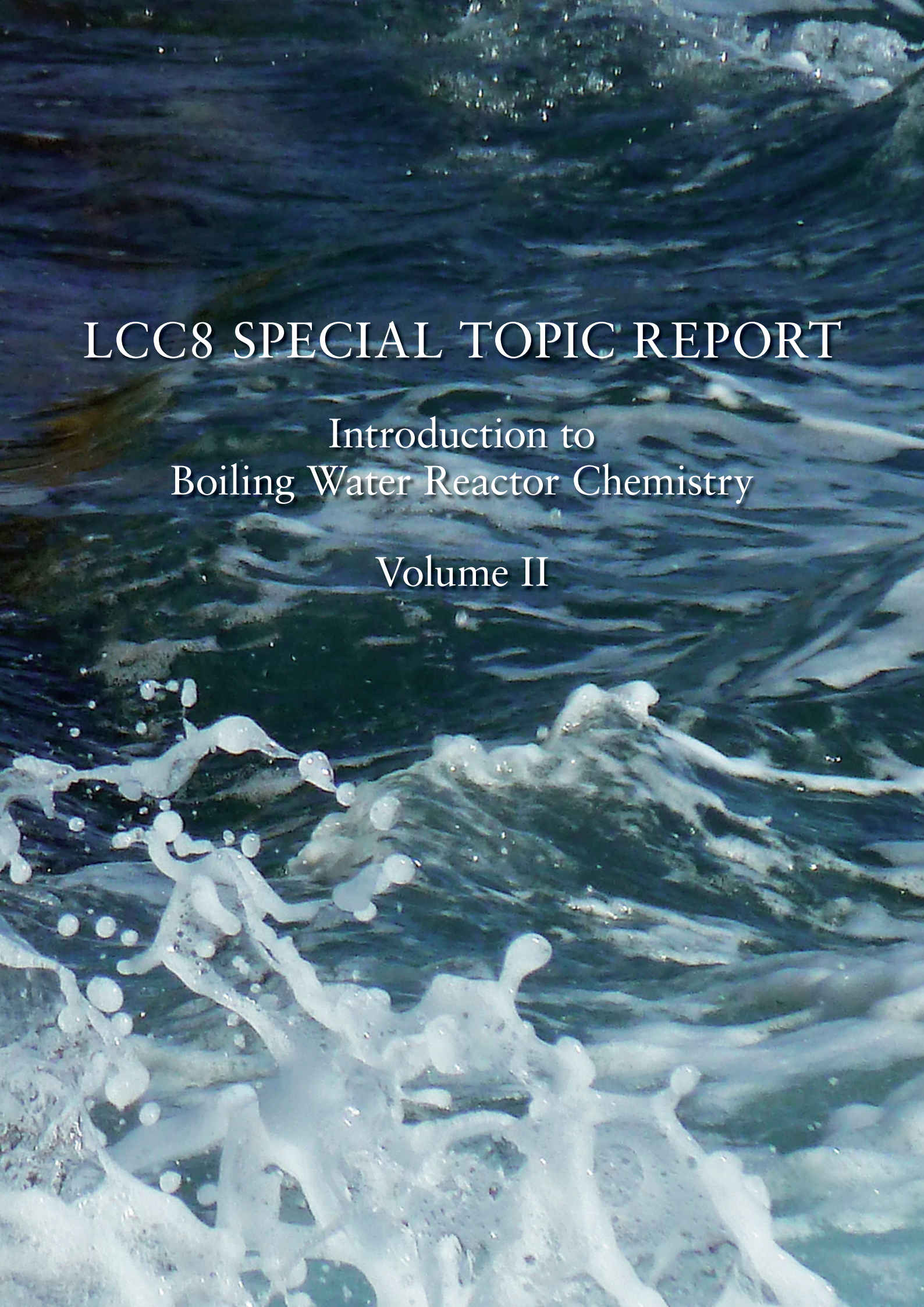

LCC8 SPECIAL TOPIC REPORT

Introduction to Boiling Water Reactor Chemistry

Volume II

Introduction to Boiling Water Reactor Chemistry

Volume II

Authors

Robert Cowan
Livermore, California, USA

Wilfried Rühle
Eppelheim, Germany

Samson Hettiarachchi
Menlo Park, California, USA

A.N.T. INTERNATIONAL®

Advanced Nuclear Technology International
Analysvägen 5, SE-435 33 Mölnlycke
Sweden

info@antinternational.com
www.antinternational.com


Ecolabelled printed matter, 441 799

Disclaimer

The information presented in this report has been compiled and analysed by Advanced Nuclear Technology International Europe AB (ANT International®) and its subcontractors. ANT International has exercised due diligence in this work, but does not warrant the accuracy or completeness of the information. ANT International does not assume any responsibility for any consequences as a result of the use of the information for any party, except a warranty for reasonable technical skill, which is limited to the amount paid for this assignment by each LCC programme member.

Contents

1 Corrosion considerations (Wilfried Rühle)

In Volume 1, the structural materials used in BWRs are reviewed as well as the applied water chemistry necessary to ensure materials integrity during a BWR's operational lifetime. In this Volume, more details about the materials and the applicable corrosion phenomena are presented.

1.1 Basic metallurgy of reactor structural materials

Considerations about the structural materials of BWR are contained in several chapters of Vol.1, especially in Section 1.4. The materials used include different types of carbon steels, low-alloy steels and austenitic stainless steels. Other structural materials are non-iron based, such as nickel-based alloys, several types of hard facing alloys and copper alloys. Zirconium alloys, which were not covered in Volume 1, are used for fuel element cladding and as structural material for the fuel bundles. An overview of zirconium alloys is given in Section 1.1.4.

1.1.1 Carbon steel

Carbon steel is made from raw iron by reduction of the carbon content to values less than 2%. Only from this concentration and lower does steel become forgeable and malleable, both when cold and warm. Higher carbon concentrations are used for cast iron. Carbon steel used in power plants usually has a carbon concentration less than 0.2%. Steel is not a homogeneous matter such as glass, but it consists of a structural arrangement of homogeneous or heterogeneous grains, which may contain inclusions or dissolved chemical elements. Carbon can be contained in steel either the dissolved state, as a hexagonal graphite phase when the carbon is >2%, or as iron carbide (Fe_3C), also called cementite. The atom ratio for cementite is 3:1, resulting in a carbon concentration of 6.67%.

There is a large variety of iron/carbon components in steel, which results in different microstructures of steel. This very complicated item can be best visualised by the iron-carbon phase diagram, showing the temperature and carbon ranges for different heat treatments, shown in Figure 1-1, Figure 1-2, Figure 1-3, Figure 1-4 and Figure 1-5.

The iron-carbon phase diagram is included in this book about BWR chemistry because of the following reasons:

- The diagram gives the chemist insight into the large variety of carbon steel types used in power plants, which have to be protected by chemical measures.
- Chemistry organizations doing metallographic examinations need the information from the diagrams for the evaluation of the grinding surface pattern.
- From the data of the diagram, the composition of the steel (e.g. content of ferrite, pearlite, cementite) can be calculated. The calculation can be made using the lever rule or using graphic solutions. Both methods are rather easy to use. Their applications, for example, can be seen in Figure 1-3.

The diagram in Figure 1-1 shows an overview of the iron-carbon diagram. It demonstrates the temperature and concentration dependence of a liquid phase (melt), its transformation to the FCC (face centred cubic) solid phase austenite at 1147°C, followed by a further transformation at 723°C to the BCC (body centred cubic) phase ferrite. Further information among others concern the correlation between the temperature of a heat and its concentration of carbon. The amount of information included in this and the following diagrams is very large. Therefore, the descriptions of the diagrams cannot be completely satisfactory. But this review should give a general overview of the contents and importance of the iron-carbon diagrams and encourage the reader to look deeper into this subject by reading specialist literature e.g. the textbooks from William D. Callister [Callister, 2008] or W. Weißbach [Weißbach, 2007].

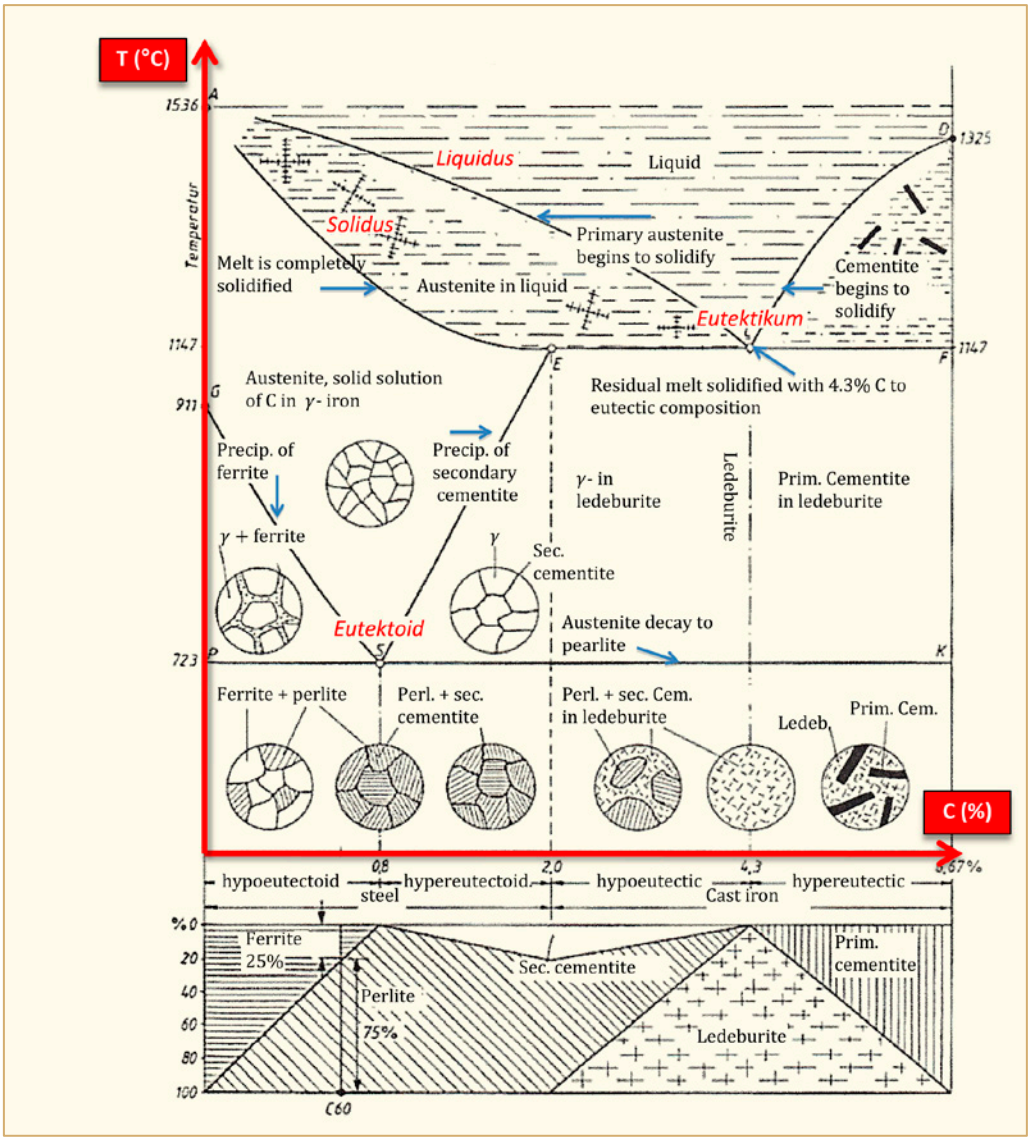

Figure 1-1: Correlation between temperature of the heat and the carbon concentration, [Weißbach, 2007].

To read an iron-carbon phase diagram one starts at the top of the diagram and go down to the bottom following a straight line parallel to the Y-axis. One starts in the melt, cuts the liquidus curve, passes an area consisting of paste-like melt plus solids, cuts the solidus curve, passes an instable solid area and ends in a stable solid area beneath 723°C. At 1147°C the melt or the paste-like mixture is changed into the eutectic. An eutectic system (eutectic is Greek for "melts easily") is a mixture of chemical compounds or chemical elements, which has a single chemical composition, which solidifies at a lower temperature than any other composition made up from the same compounds.

The diagram in Figure 1-2 shows areas of stability or meta stability for different phases and the changes in concentrations during the solidification of steel. Of special interest is the eutectoid transformation of the BCC solid austenitic phase. At 723°C pearlite is formed, which has a striped microstructure consisting of ferrite (α-ferrite) and cementite (Fe_3C).

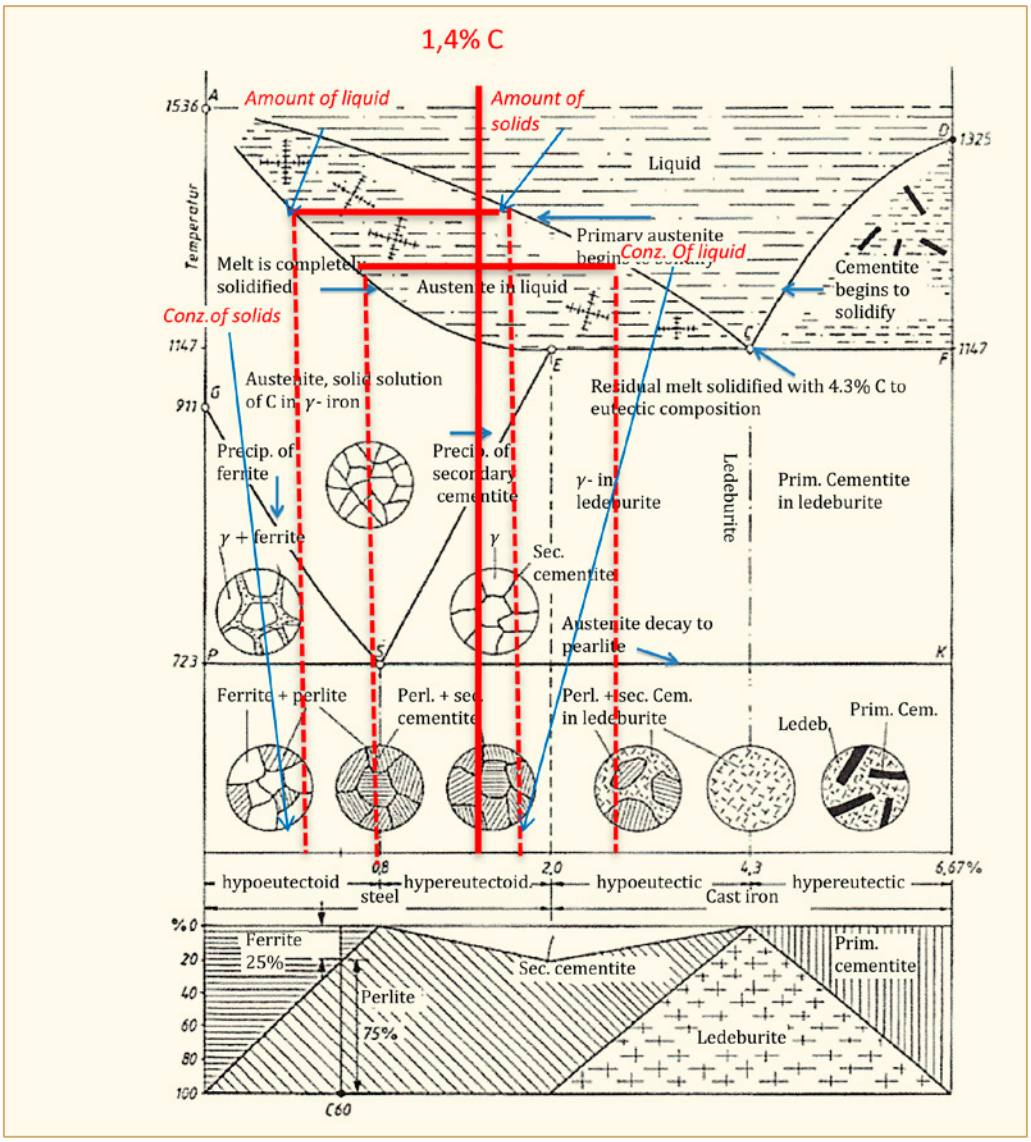

Figure 1-2: Iron-carbon diagram with microstructures and areas of stability and meta stability of different phases, [Weißbach, 2007].

These phases are characterized as follows:

- α–ferrite, a solid solution of carbon in body centred cubic (BCC) iron stable at room temperature:
  - The maximum solubility of carbon in α – ferrite is 0.022% w/w at 723°C
  - It transforms to face centred cubic iron (FCC) or γ-austenite at 911°C
- γ- austenite, a solid solution of C in face centered cubic (FCC) Fe:
  - The maximum solubility of C is 2.05% w/w at 1147°C
  - It transforms to BCC δ-ferrite at 1392°C (not from technical interest)
  - It is not stable below the eutectic temperature (723°C) unless cooled rapidly

- δ- ferrite, a solid solution of C in BCC Fe:
  - It has the same structure as α-ferrite
  - It is stable only at high temperature above 1392°C
  - It melts at 1536°C
- Fe_3C, iron carbide or cementite:
  - This intermetallic compound of carbon and iron is metastable, it remains as a compound indefinitely at room temperature, but decomposes very slowly into α-Fe and C at 650 – 700°C.
- Fe-C, as a liquid solution

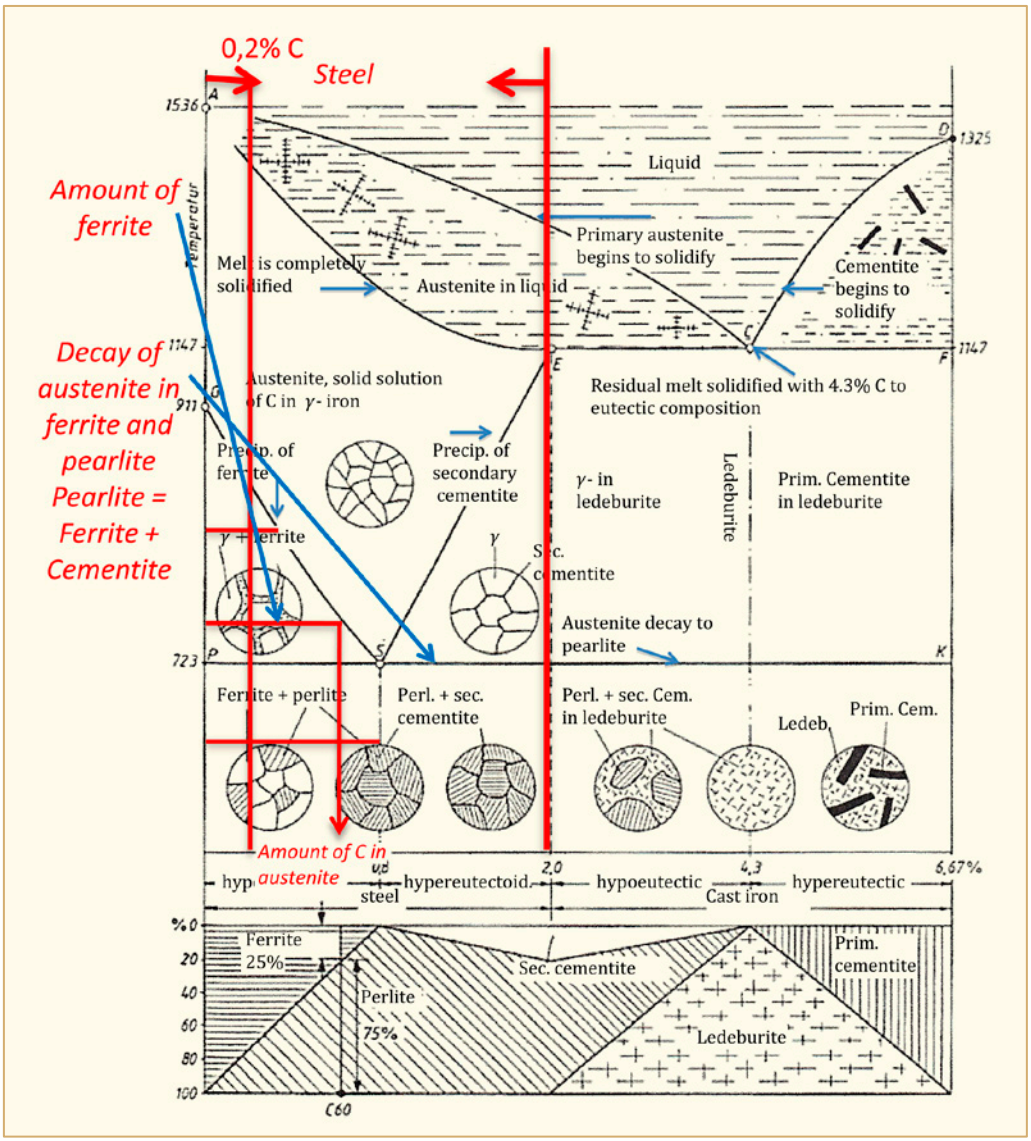

Figure 1-3: Steel with carbon content less than 0.8% is called hypoeutectoid, consisting from pearlite and ferrite. At 723°C austenite decays into ferrite and pearlite, [Weißbach, 2007].

The amount of each component in a two phase alloy can be calculated by the lever rule. The horizontal red bars in Figure 1-3 show the amount of ferrite and pearlite during the slow cooling down process for a definite carbon concentration. The lower part of Figure 1-3 shows a graphic method for determination of the alloys composition.

The background concerning the austenite decay can be explained as follows: Austenite is, as mentioned before, a solid solution of carbon in face centred cubic iron (FCC) with a maximum solubility of 2.05% w/w. With decreasing temperature the solubility of carbon decreases to 0.8% w/w at 723°C. Below this temperature it decays to ferrite, a solid solution of carbon in body centred cubic iron (BCC) with a maximum carbon solubility of only 0.022% w/w. Thus carbon previously dissolved in austenite has no more space in the new crystal lattice. So it forms a new phase with iron, iron carbide or cementite. This mixture is called pearlite.

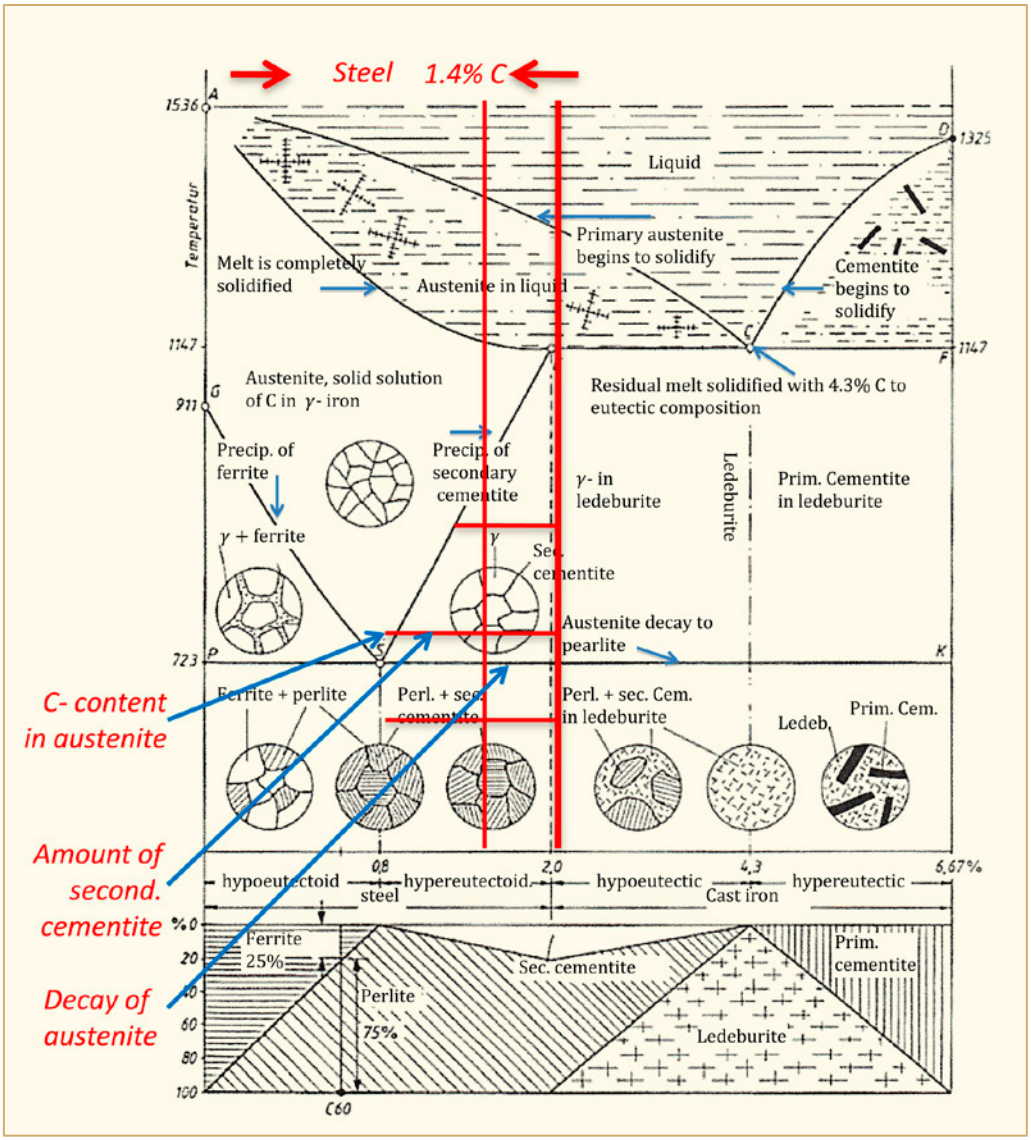

Figure 1-4 Steel with 0.76 to 2.14 wt% C is called hypereutectoid containing pearlite and secondary cementite; at the eutectoid point, pearlite is generated (ferrite and cementite), [Weißbach, 2007].

When the carbon concentration in the melt is in a region between about 0.8 and 2% w/w, a slow cooling process forms the products shown in Figure 1-4. In addition to pearlite, which is produced at the eutectoid point, secondary cementite is formed.

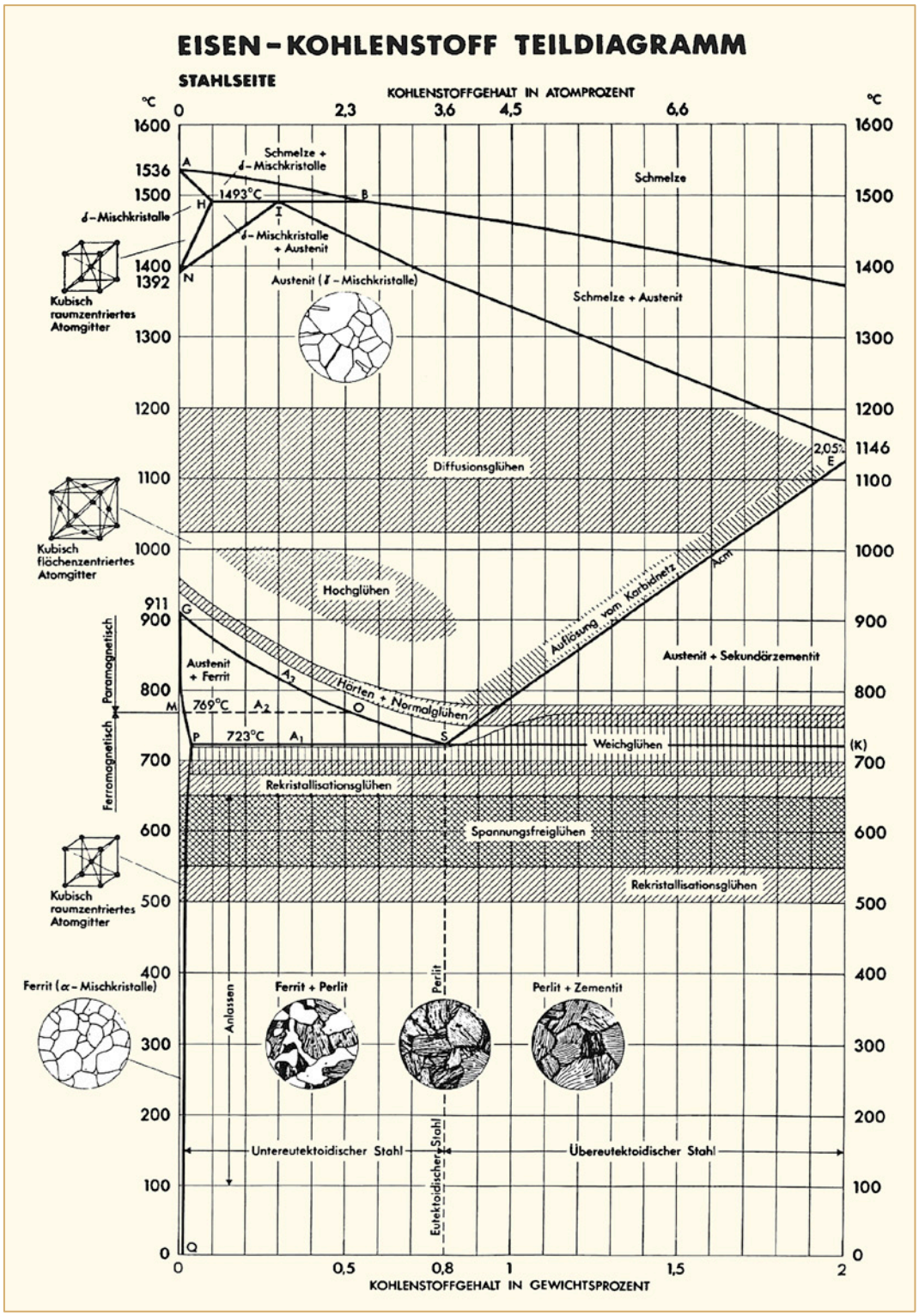

Figure 1-5: Iron-carbon phase diagram with microstructures showing the steel side only and the region of pure ferrite being nearly free from carbon because of the BCC crystallisation (Carbon forms a solid solution with γ-, α-, and δ-phases of iron as an interstitial impurity). The maximum carbon solubility in body centred cubic (BCC) α- ferrite is limited (0.022% w/w at 723°C), as BCC has relatively small interstitial positions. The maximum solubility in FCC austenite is 2.05% w/w at 1147°C, because the face centred cubic structure FCC has larger interstitial positions), [Weißbach, 2007].

Figure 1-5 shows the steel part of the iron-carbon diagram only. It additionally shows the region of pure α –ferrite, which has only a very small dissolved carbon content because of its BCC structure. The cubes on the left edge of the diagram show the FCC and the BCC structures. The upper part of the diagram between 1536°C and 1392°C with the area for δ-ferrite is for theoretical information only and has no practical relevance.

1.1.1.1 Eutectic and eutectoid points

A melt crystallizes to γ- mixed crystals (coming from the lower carbon side of the diagram with C <0.8%) and Fe_3C (coming from the carbon rich side of the diagram with C >0.8%) following the solidus curves continuously changing the carbon concentration in the melt. At the eutectic point at 1147°C the melt crystallizes with a constant carbon concentration at 4.3% w/w C. A similar situation exists at 723°C and 0.8% w/w C. But in this case a transition in the matrix takes place changing its structure from γ-austenite to α-ferrite from solid phase to solid phase. Therefore, this point cannot be called eutectic point. Alternatively it is called eutectoid point. At this point γ-iron (austenite) with 0.8% w/w C decays into α- ferrite (0.022% w/w C) and Fe_3C. This phase is called pearlite, a fine striped lamellar mixture of α-ferrite and cementite (see the encircled pictures in Figure 1-5).

In case the metal is cooling down slowly, the two phases generated at the eutectoid point form pearlite, which is a lamellar product. The layers alternating consist from α-ferrite and Fe_3C (Figure 1-3 and Figure 1-5).

In case there is a composition from the left side of the eutectoid point (Figure 1-3) with less carbon than 0.8% w/w, the hypoeutectic area, we get a product consisting from pearlite and residual α- ferrite. The residual α-ferrite is also called "proeutectoid α-ferrite". On the right side of the eutectoid point (0.8 – 2.05% w/w C), in the hypereutectoid area, one gets pearlite, proeutectoid α- ferrite, and additional Fe_3C (cementite). With increasing Fe_3C–concentration, the hardness of the metal is increasing.

1.1.2 Stainless steel

The composition and behaviour of the austenitic stainless steel types used in BWRs has been described in Vol. 1. The focus is on sensitization of the materials and the countermeasures, low carbon and/or stabilization.

1.1.3 Nickel-based alloys

The nickel based alloys (sometimes called super-alloys or high-performance alloys) that are used in BWRs and PWRs are nickel-chromium-iron alloys with high mechanical strength and creep resistance. They retain these properties up to fairly high temperatures. For reactor applications, their excellent corrosion behaviour is very important and at some locations it is essential. These alloys were developed especially for jet engines and for the chemical industry, because of their resistance against aggressive chemicals.

In nuclear reactors their high temperature features – high strength, creep resistance, fatigue life, phase stability and oxidation stability - don't play a main role, as the highest possible operating temperatures in light water reactors are below 350°C. Their normal industrial application is based on their corrosion resistance against aggressive water environments. Their use under BWR-conditions has only limited applications and includes varies welding procedures. Some details about these items are reviewed in Section 1.5. High strength components, such as bolts and springs, are also made from nickel-based-alloys, which are further optimized by additional alloying elements.

Nickel based alloys in nuclear reactors are predominantly known by the trademark "Inconel". Table 1-1 shows the commonly used Inconel variants and their chemical composition. In PWRs the main areas of their use are the steam generators (Inconel 600 and later 690; in German PWRs Incoloy 800, a high alloyed stainless steel is used). In BWRs, nickel based alloys are usually only used for smaller components or as transition weld "butter materials" for carbon/low alloy steel to stainless steel welds. Nickel based alloys are also used as weld filler materials, such as Alloy 82 and 182.

Table 1-1: Examples for nickel based alloys (Inconel) in Light Water Reactors.

Element (% by mass)																
Inconel	**Ni**	**Cr**	**Fe**	**Mo**	**Nb**	**Co**	**Mn**	**Cu**	**Al**	**Ti**	**Si**	**C**	**S**	**P**	**B**	**others**
600	72.0	14.0-17.0	6.0-10.0				1.0	0.5			0.5	0.15	0.25015			
690	58.0 min	27.0-31.0	7.0-11.0			Incl. in Ni	0.5 max	0.5 max			0.5 max	0.05 max	0.015 max			
X-750	70.0	14.0-17.0	5.0-9.0		0.7-0.2	1.0	1.0	0.5	0.4-1.0	2.25-2.75	0.5	0.08	0.01			
182	59.0	13.0-17.0	10.0 max		1.0-2.5 incl. Ta	Incl. in Ni	5.0-9.5	0.5 max		1.0 max	1.0 max	0.1 max	0.015 max	0.03 max		0.5 max
82	67.0 min	18.0-22.0	3.0 max		2.0-3.0 incl. Ta		2.5-3.5	0.5 max		0.75 max	0.5 max	0.1 max	0.015 max	0.03 max		0.5 max
Incoloy	**Ni**	**Cr**	**Fe**	**Mo**	**Nb**	**Co**	**Mn**	**Cu**	**Al**	**Ti**	**Si**	**C**	**S**	**P**	**B**	**others**
800	30.0-35.0	19.0-23.0	39.5 min						0.15-0.6	0.15-0.6		0.1 max				
ANT International, 2012																

1.1.4 Zirconium alloys

A comprehensive handbook dealing with zirconium alloys for fuel elements and other reactor core components is available from ANT as the "Fuel Material Technology Report (FMTR) Volume I through IV. The following considerations are very limited and give only a short introduction into this subject.

Free accessible literature about Zircaloy 2 and Zircaloy 4, dealing with the composition, the corrosion behaviour, the physical properties, the mechanical properties, the nuclear properties, the radiation effects and the metal water reactions is available in ORNL-3281 [Whitmarsh, 1962]. Although the report is very old, the included information is informative and is still valid.

Zirconium metal is very resistant against corrosion in acid or alkaline environment because of its immediate passivation by a zirconium oxide layer. The pure metal is soft, ductile and malleable, but by addition of small amounts of other metals, the mechanical and chemical properties can be improved. A very important family of zirconium alloys is known by the trade-mark "Zircaloy". Zirconium and Zircaloy have a very low absorption cross-section for thermal neutrons. This makes it very suitable for use in nuclear reactors for the fabrication of fuel rods and other reactor internals.

The use of zirconium in nuclear reactors goes back to the time immediately after World War 2 and the development of nuclear reactors for ship propulsion. The advocator of zirconium as a cladding tube for the nuclear fuel was Admiral Hyman Rickover, who pushed the development and production of Zircaloy against heavy opposition [Duncan, 2001].

Zircaloy-2 is used in BWRs as fuel cladding. Zircaloy-2 is an alloy of zirconium and tin, with smaller amounts of Fe, Ni and Cr. The nuclear grade product specification is in Table 1-2. The analysis values for Zircaloy 2 are from different sources published in 1962 and recently. The only difference in the currently specified alloy is the concentration value for oxygen. The alloy for the Russian BWR, the RBMK is predominantly a zirconium alloy, containing 1% niobium. The relevant difference between Zircaloy 2 and Zircaloy 4 is the elimination of nickel from the Zircaloy 4 specification. The reason for the low nickel requirement is to improve the resistance to hydrogen absorption into the matrix catalysed by nickel in the reducing environment of PRWs.

Table 1-2: Composition of Zircaloy-2 (old data, new data, RBMK data) in comparison to Zircaloy-4 [Witmarsh, 1952].

Alloy	Sn%	Nb%	Fe%	Cr%	Ni%	O%	Source
Zircaloy-2	1.2-1.7	-	0,07-0.2	0.05-0.15	0.03-0.08	0.1-0.014	[AWiki]
Zircaloy-2	1.2-1.7	-	0,07-0.2	0.05-0.15	0.03-0.08		[ORNL-3281]
Zircaloy-4	1.2-1.7	-	0.18-0.24	0.07-0.13	-	0.1-0.14	[AWiki]
E-110 RBMK	-	0.9-1.1	0.14	<0.003	0.0035	0.06-0.07	[AWiki]
M5		1					[Zwicky, 2006]
							ANT International, 2012

During the last few years, the performance requirements for fuel cladding have been increased due to economic and safety reasons. As can be seen from Table 1-2, the materials have not generally changed. The materials have been optimized by:

- Tighter specification for some impurities and varying some alloying contents within the specified range.
- Optimization of the metal crystal orientation for cladding ductility using the cold pilger (or rocking) process instead of the more commonly used drawing process to produce tubing.
- Optimization of the size of intermetallics for BWR cladding corrosion resistance. The size and uniformity of the $Zr(Fe,Cr,Ni)_n$ intermetallics, or second phase particles, affects BWR corrosion behaviour.
- Optimization of the claddings for improved power ramp PCI resistance (a semi-pure zirconium inner liner with different small alloy additions).

More details about the Zircaloy improvement is available from AWiki http://previewwiki.antinternational.com/wiki/Fuel_Assembly_Materials [Strasser et al, 2010] and from the publications within the ZIRAT program from ANT International.

1.2 Corrosion fundamentals

We have seen in Volume 1 that the interaction of metals and water is a fundamental issue for design and operation of thermal power plants. In the following chapters the mechanisms for the dissolution of metals in water is discussed and the reactions of the metal ions with water to corrosion products and protective layers are described.

As iron is the most important and mostly used structure material and as its corrosion chemistry is best known, the following considerations about metal and water are made using iron as the example.

1.2.1 Iron in pure water

It is well known that bare iron in water releases iron ions into the water. In case of oxygen free water the species released are Fe^{2+} ions. The driving force for this conversion from the solid state to the dissolved status is the increase in entropy according to the second law of thermodynamics, which says:" The entropy of an isolated system not in thermal equilibrium always increases". Therefore, isolated systems spontaneously evolve towards thermal equilibrium, which is the state of maximum entropy of the system. In case of iron, the metal is fixed as ions in the crystal lattice surrounded by an electron cloud. This is a status of high order and so of low entropy. Changing into the dissolved status will diminish order and so increase the entropy of the closed system.

The electrons remaining in the crystal lattice result in a negative electric load of the metal. This negative load of the metal and the positive load of the water by the positive ions generate an electric field. If the electric field is so high that the ions cannot work upwards against it, the dissolution of the metal comes –at the first view- to an end. The positively charged ions and the negatively charged metal generate an electric double layer and consequently a potential difference, which is called "electrode potential". The electrode potential is characteristic for a certain metal, but it depends also on other physical and chemical parameters, such as the temperature and the concentration of ions of the same metal added to the solution in form of salts. If the salt or ions concentration is high, the dissolution process can be reversed by precipitation of metal ions at the metal surface. Precipitation of positively charged metal ions at the metal surface could switch the electric metal load from negative to positive, and so change the direction of the electric field between the metal and the residual anions in the opposite direction.

1.2.2 Measurement of the electrode potential

The direct measurement of a single electrode potential is not possible because there is no zero point available. So the measurement has to be done in comparison to a second electrode. This should not be another metal electrode, because that one would also depend on the ion concentration in the solution. What is needed is an electrode, which does not interfere with the metal ions to be measured. The best solution to solve this problem is using the "standard hydrogen electrode (SHE)" as a reference electrode. The single potential of the SHE is generated by the reaction:

$$H_2 \leftrightarrow 2H^+ + 2e^-$$

The hydrogen electrode is a redox electrode using platinised platinum dipped in an acidic solution through which pure hydrogen gas is bubbled. The activity concentration for the hydrogen ions a[H^+] must be 1mol/kg, the hydrogen pressure 1013 mbar and the temperature 298.15 K. It can easily be seen that working with such an electrode is not easy, as keeping the mentioned parameters constant is difficult. It is much easier to use a commercial reference electrode with a more constant potential. Such an electrode is the "saturated calomel electrode", which has the potential E_H = 0.252 Volt at 25°C. If the potential of any electrode is measured against the calomel electrode at 25°C, to the measured value 0.252 V have to be added.

The electrode potential of the hydrogen electrode can be calculated by Nernst equation. The equation for a gas electrode consists of a concentration dependant term and a pressure dependant term:

$$E_H = E_H^0 + \frac{RT}{F} \ln a_{H^+} - \frac{RT}{2F} \ln p_{H_2}$$

R = universal gas constant

T = absolute temperature

z = valance of the metal ions determining the potential

F = Faraday constant

a_{H^+} = activity concentration of hydrogen ions

p_{H_2} = partial pressure of hydrogen gas

The standard electrode potential or normal potential is obtained by equalising the hydrogen ion activity concentration and the hydrogen partial pressure to 1. At this condition, $E_H = E_H^0$ and this defines zero Volts on the Standard Hydrogen Scale. Note that the standard hydrogen potential, E_H^0, is defined as zero at all temperatures.

The potential of a metal electrode, $\mathbf{E}_{Me/Me^{z+}}$, can also be calculated by the Nernst equation:

$$\text{for:} \quad Me \leftrightarrow Me^{+z} + ze^{-}$$

$$\mathbf{E}_{Me/Me^{z+}} = E_{Me}^0 + \frac{RT}{zF} \ln m_{Me^{z+}}$$

z = valence of the metal ions

$m_{Me^{z+}}$ = concentration of the metal ions

If we solve this equation for the metal ions $m_{Me^{z+}} = 1$mol/l, we get "zero" for the second term and so $\mathbf{E}_{Me/Me^{z+}} = E_{Me}^0$, where E_{Me}^0 is the potential of the metal electrode against the standard hydrogen electrode. This can be seen as a standardisation and this potential is called "normal potential or standard potential".

Table 1-3 shows a series of measured normal potentials for the most important corrosion related parameters.

Table 1-3: Normal potentials for some corrosion relevant redox systems on the Standard Hydrogen Electrode scale, E_H^0 [Volt], after [Hömig, 1971].

Electrode	E_H^0 [Volt]	Electrode	E_H^0 [Volt]
Li^+/Li	-3.00	Co^{2+}/Co	-0.28
Rb^+/Rb	-2.97	Ni^{2+}/Ni	-0.236
K^+/K	-2.922	Sn^{2+}/Sn	-0.136
Cs^+/Cs	-2.92	Pb^{2+}/Pb	-0.126
Ba^{2+}/Ba	-2.92	Fe^{2+}/Fe	-0.045
Sr^{2+}/Sr	-2.89	Cu^{2+}/Cu	+0.345
Ca^{2+}/Ca	-2.84	$½\ O_2/2OH$	+0.401
Na^+/Na	-2.713	Cu^+/Cu	+0.52
Mg^{2+}/Mg	-2.38	$J_2/2J^-$	+0.536
Al^{3+}/Al	-1.66	$Hg_2^{2+}/2Hg$	+0.798
Mn^{2+}/Mn	-1.05	Ag^+/Ag	+0.799
Se/Se^{2-}	-0.78	Pd^{2+}/Pd	+0.83
Zn^{2+}/Zn	-0.763	Hg^{2+}/Hg	+0.854
Cr^{3+}/Cr	-0.71	$Br_2/2Br^-$	+1.066
Cr^{2+}/Cr	-0.56	Pt^{2+}/Pt	+1.2
S/S^{2-}	-0.51	$Cl_2/2Cl^-$	+1.359
Fe^{2+}/Fe	-0.441	Au^{3+}/Au	+1.42
Cd^{2+}/Cd	-0.401	Au^+/Au	+1.7
Tl^+/Tl	-0.336	$F_2/2F^-$	+2.85
			ANT International, 2012

It is important to know that the values from Table 1-3 are only from theoretical interest, but not for practical use. The reasons are that conditions in the real water are different from those in the laboratory and chemical and metallurgical conditions between the laboratory specimen and technical metal samples are different too. H.E. Hömig has expressed this awareness as follows:

"Which potential arises at an electrode doesn't depend on the kind of metal the electrode is made from, but from the process taking place at the surface of the electrode".

To demonstrate this, Hömig shows a real electromotive chain made by measurements in moving, air saturated artificial seawater at pH 7.5, 25°C and 1013 mbar.

Table 1-4: Standard potentials (electromotive chain) in artificial seawater, after [Hömig, 1971].

Metal in the solution	E_H [Volt]
Sn	-0.809
Fe (technological)	-0.45 to -0.30 (depending on the iron sample)
Zn	-0.248
Pb	-0.259
Cu	+0.010
Ni	+0.046
Ag	+0.149
ANT International, 2012	

This table shows that under practical conditions several metals have changed their positions they had under laboratory conditions. Changing the chemical conditions in the water can easily change these values. Good examples are changing the pH by ammonia addition.

Till now the dissolution model described in 7.2.1 stops after having reached equilibrium in the form of a double layer from negative charged metal and a positive charged ion cloud in the water. The generated electric field prohibits further dissolution of the metal. We know from experience that in reality corrosion doesn't stop as theoretically expected, because there is another mechanism which destroys the electric field. This is possible only, if a second electrode exists with a different electrode process. While the first electrode process, the anodic corrosion, is the reaction:

$$Fe \rightarrow Fe^{++} + 2e^{-}$$

The second electrode process in oxygen free water should be:

$$2H^{+} + 2e^{-} \rightarrow H_2$$

While the first sub-process is delivering electrons, the second sub-process is consuming electrons, and this keeps the corrosion going. This means that electrochemical corrosion can proceed only if two or more electrode processes are running. While one process is delivering electrons, the second is consuming them.

This combination of two electrodes is called an "electrochemical cell" or "corrosion cell". The electrode delivering the electrons is called the "anode" and the electrode consuming the electrons is called the "cathode". The dissolution (corrosion) of the metal surface (starting at surface imperfections) occurs at the anode while the cathode is not corroded.

The electrons migrate from anode to cathode, meaning that the cathode must have a higher potential than the anode. In pure water the highest electrode potential is the reduction of hydrogen ions to hydrogen gas. Therefore metals with higher potential than the hydrogen electrode cannot corrode in oxygen free water. In other words: In oxygen free pure water, metals can only be dissolved by electrochemical corrosion, if its anodic dissolution potential is lower than the potential of the hydrogen electrode. This situation is only valid in absence of oxidising agents. In presence of oxidising agents, metals nobler than H^+ ions are also dissolved. The nobler a metal is, the stronger must the oxidising agent be to dissolve it.

In our model we connect a less noble metal, for example iron, to a more noble metal, such as copper. For this case, iron is dissolved and hydrogen is produced at the nobler electrode. But we know from practical experience that iron corrodes without presence of an external electrode. The question is: where is the cathode? The only answer is that anode and cathode must both be on the iron electrode. If we look at the metal surface with a microscope we see the reason very easily. The metal is not homogenous like glass, but it has a polycrystalline structure and it is inhomogeneous by the fabrication process. This enables the metal to have anodic and cathodic areas on the same surface close together. Furthermore anodic and cathodic areas can change their location and so result in uniform corrosion.

We have now seen that the electrochemical corrosion of metals depends on local cells on the metal surface, whereas metal is dissolved at the anode and hydrogen ions are discharged at the cathode. Obviously the concentrations of hydrogen ions and metal ions in the solution influence the potential difference of the local cell. This can easily be calculated by the Nernst equations.

Figure 1-6 shows the potential of the hydrogen electrode for different hydrogen partial pressures and different hydrogen ion concentrations. The hydrogen ion concentration (activity) determines by definition the pH, whereas for $a_{H^+} = 1$, the pH = 0. If the partial pressure for hydrogen is 1 bar, than the potential $E_H = E_H^0$ is zero. At higher pH-values the hydrogen ion concentration decreases and therefore decreases the potential. The same behaviour shows the hydrogen partial pressure.

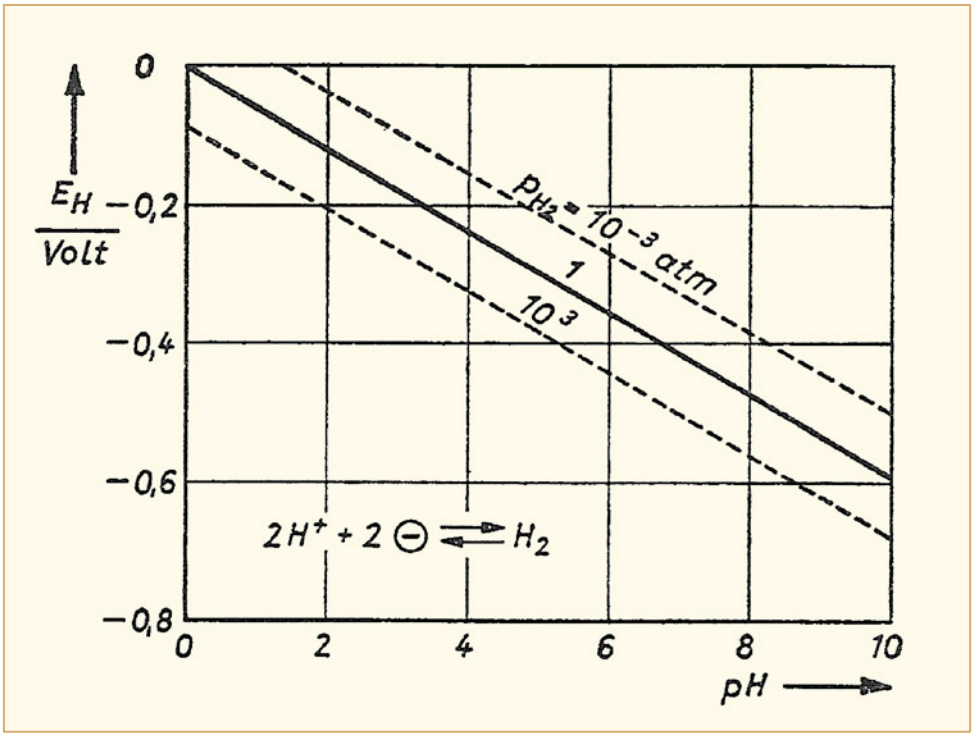

Figure 1-6: Potential of the hydrogen electrode [Hömig, 1971].

The potential of a metal electrode, using the example of iron, depending on the Fe ion concentration in solution and the pH is shown in Figure 1-7. According to the Nernst equation, the potential of the Fe/Fe^{++} cell is independent from the pH-value, meaning that in a potential-pH diagram, the potential- pH lines are horizontal. Because the solubility of Fe^{++} is limited in correlation to the pH, there is a maximum value for each concentration at the point where $Fe(OH)_2$ precipitates. The precipitation points in correlation to potential- and pH-values are a straight line, shown in Figure 1-7 as a "Saturation line". It is important to know that there cannot be an iron cell with a potential above this line.

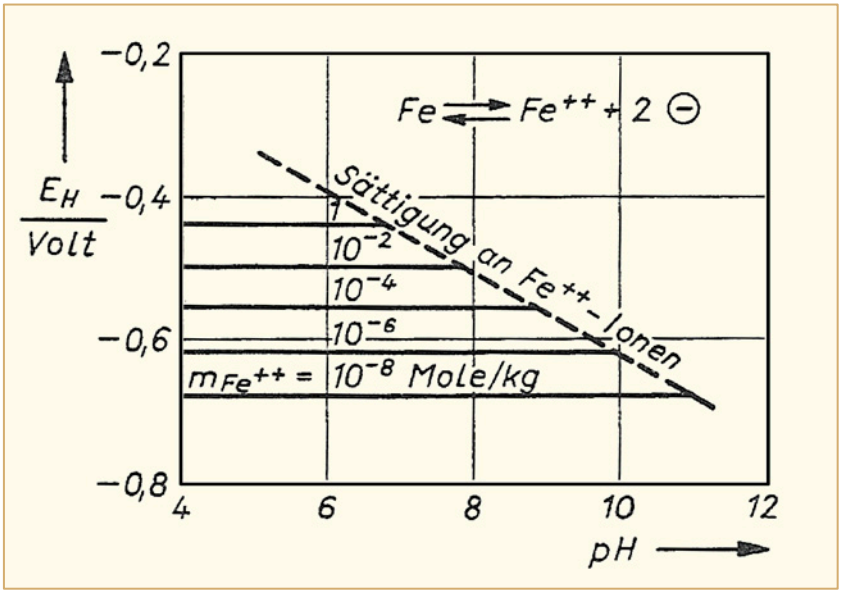

Figure 1-7: Potential of the Fe/Fe^{2+} - electrode [Hömig, 1971].

The diagrams for hydrogen potential and for the metal-metal ion potential can be combined in one diagram (Figure 1-8).

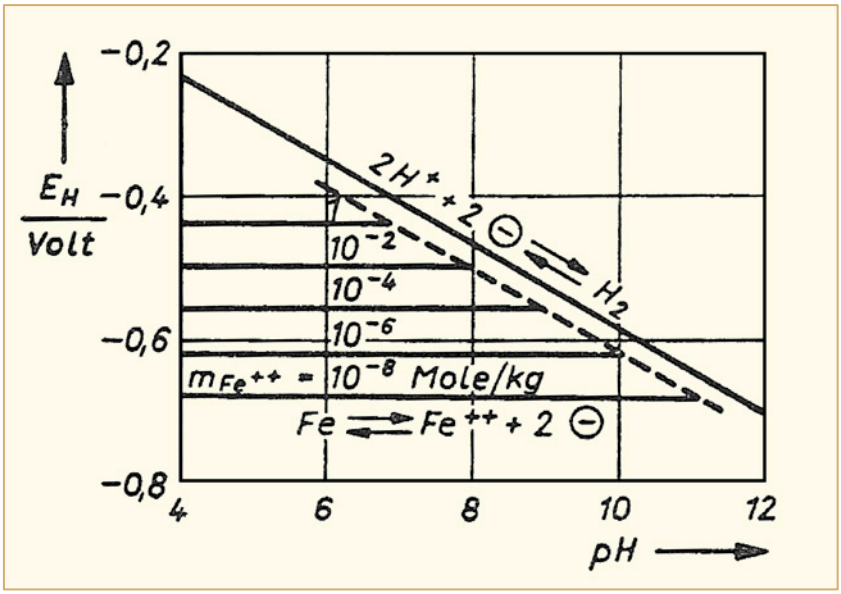

Figure 1-8: Equilibrium diagram for iron – water (in absence of oxygen) [Hömig, 1971].

We can see that in the whole pH region the potential of the Fe/Fe^{++} cell is below the hydrogen cell. This means that under the described conditions iron inevitably will be dissolved by formation of hydrogen. In stagnating water, the iron ions concentration would be rather low, but in flowing water iron would be dissolved continuously. In stagnating water we would have small dissolution, in flowing water we would have high dissolution, depending on the flow velocity. The system iron and water is thermodynamically unstable.

We will see later that the thermodynamic instability of iron in water is a theoretical problem only, because the formation of protective layers helps us to control and reduce the iron solubility. Another measure to reduce iron corrosion is using surface inhibitors. These can be inorganic chemicals like phosphates and silicates, which react with iron to form insoluble products, or organic molecules such as organic amines, which are adsorbed at the metal surface and so hinder its dissolution. Inhibitors are predominantly used in cold water systems with great success, but this application is outside the scope of this book.

For the scientific explanation of the behaviour of protective layers more theoretical background in electrochemistry is necessary. Important items are the different types of polarisation of the cells and the corrosion current. Especially current density- potential curves can help to explain corrosion mechanisms. More information about these items can be taken from special literature about electrochemistry and corrosion.

1.2.3 Protective layers and passivity

A beneficial side effect of corrosion can be the formation of corrosion products which can generate protective layers at the metal surfaces, preventing the metal from further corrosion. Such mechanisms make the technical use of the majority of metals and metal alloys possible.

The most obvious agents, which can form protective layers are OH^- -ions, which react in neutral water with iron to insoluble Fe $(OH)_2$ and so inhibit the dissolution process. As iron (II) hydroxide is thermodynamically unstable, at room temperature it is slowly converted to magnetite, Fe_3O_4. At low temperature magnetite is not a good protective layer, so the protective agent is still the hydroxide. But at high temperatures (>200°C), the transformation occurs very quickly and the hydroxide is only a short lived intermediate product. The reaction

$$3\ Fe\ (OH)_2 \rightarrow Fe_3O_4 + H_2 + 2H_2O$$

is called Schikorr reaction. The formation of magnetite is promoted by high pH-values, but it is also stable in neutral or in mild acidic environment. Magnetite is covered in more detail in later chapters.

1.2.3.1 Influence of oxygen on the corrosion of iron

Till now, we have described the corrosion of iron in oxygen free water. It is easy to understand that aside from the conditions in an autoclave, it is nearly impossible to operate a technical system without the influence of oxygen. In the presence of oxygen, the formation of a local oxygen cell working as a cathode has to be considered. In BWRs, there is continuous formation of oxygen by radiolysis, which is then distributed over all water and steam containing systems (Vol. 1, 2.1).

For a better understanding of the behaviour of oxygen in water, here are some facts about its solubility in could and hot water. At room temperature (25°C), water in contact with air will contain about 8 mg/ kg of dissolved oxygen. With increasing temperature, if boiling is avoided by corresponding pressure increases, the solubility decreases until it reaches its minimum at about 115°C. That we have zero solubility at 100°C under one atmosphere of pressure is only an effect of boiling. Degassing by boiling is completely independent from the solubility of oxygen and other non-condensable gases. From 115°C and hotter, the solubility increases with temperature (and pressure). So, high temperature water can have high concentrations of dissolved oxygen.

Oxygen in water can easily accept electrons by the reaction:

$$O_2 + 4e^- + 2H_2O \leftrightarrow 4\ OH^-$$

The equilibrium potential for this cell is determined by the OH^- concentration and the partial pressure of oxygen. The normal potential of this electrode is 0.4 Volt (Table 1-1) and the pH dependency can be calculated with the Nernst- equation:

$$E_{O_2/OH^-} = E^0_{O_2/OH^-} + \frac{RT}{F} \ln a_{OH^-} - \frac{RT}{4F}\, ln\, p_{O_2}$$

The graph of this curve is shown in Figure 1-9. One can see that the equilibrium potentials are parallel and that the potential of the oxygen electrode is 1.2 Volt higher than that of the hydrogen electrode. This big difference makes it clear that oxygen can promote the electrochemical corrosion easily. The area between the two potential lines is the region where water is thermodynamically stable.

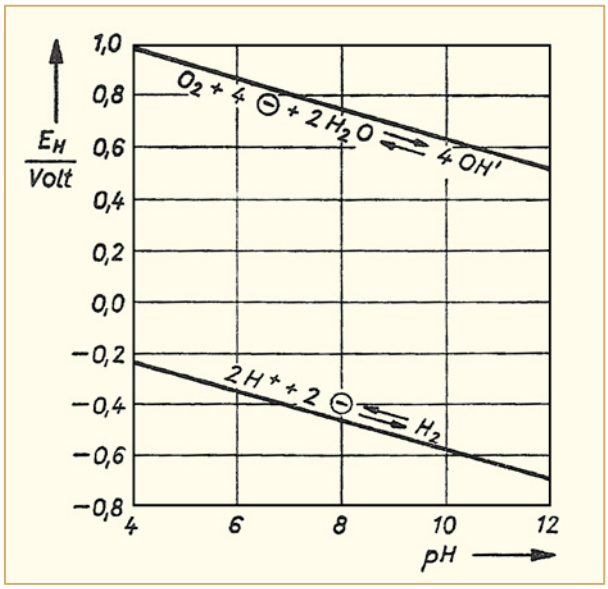

Figure 1-9: Equilibrium potential for the oxygen- and hydrogen-cell or "stability diagram for water" [Hömig, 1971].

1.2.4 Pourbaix diagrams

Pourbaix diagrams are potential-pH- diagrams, showing the existence regions for a metal and their oxides, hydroxides and ions in aqueous environment in a stable equilibrium condition. Pourbaix diagrams are calculated using the Nernst equation:

$$\text{for:}\quad Me \leftrightarrow Me^{+z} + ze^-$$

$$E_{Me/Me^{z+}} = E^0_{Me/Me^{z+}} + \frac{RT}{zF} \ln m_{Me^{z+}}$$

$E_{Me/Me^{z+}}$ is the potential related to the hydrogen electrode between solution and metal electrode for equilibrium conditions. In case of a redox-reaction, R, according to the equation:

$$aA + bB + ne \Leftrightarrow pP + qQ$$

the Nernst potential-equation is:

$$E_R = E^0_R + \frac{RT}{nF} \ln [A^a \times B^b / P^p \times Q^q\ ].$$

2 Stress corrosion cracking mitigation (Samson Hettiarachchi)

The BWR was originally designed to operate with high purity water, but many began to utilize small additions of zinc to control shutdown/drywell dose rates. Modern day BWRs typically operate with a reactor water conductivity of about 0.08 μS/cm due to the presence of zinc ions in the reactor water. However, the presence of other undesirable ionic species may increase the reactor water conductivity thereby increasing the propensity of structural materials like stainless steels and nickel alloys to undergo intergranular stress corrosion cracking (IGSCC). The impact of many of these ionic impurities on IGSCC was covered in Section 2 of the LCC7 report. The intent of this Section is specifically to show the importance of minimizing chlorides and sulphates on the IGSCC mitigation of BWR structural materials. An additional objective of this Section is to describe the IGSCC mitigation technologies employed by the BWR industry.

2.1 Importance of minimizing ionic impurities – chlorides and sulphates

2.1.1 Importance of minimizing chlorides

Chloride ion is detrimental to the SCC resistance of BWR materials as shown by many authors [Gordon 1980], [Hishida & Nakada, 1977], [Hubner et al, 1971], [Congleton et al, 1990] and [König et al, 2004]. Research has been performed in Sweden using reversing DC potential drop (DCPD) crack growth rate studies on Type 304 stainless steel and Alloy 182 weld metal in simulated NWC (500 ppb dissolved oxygen) and HWC (2-8 ppb dissolved oxygen) environments in the presence of chloride ions [König et al, 2004]. As shown in Figure 2-1 and Figure 2-2, increasing chloride concentration results in increased crack growth rate acceleration in both NWC and HWC environments for furnace sensitized Type 304 stainless steel [Gordon & Garcia, 2010].

In general, the type of cracking observed with Chloride is transgranular (TGSCC) as opposed to IGSCC that is commonly observed with sulphate impurities. It is expected that the crack growth rate with chlorides would be lower compared to that with sulphates. In addition to TGSCC, chloride ion is well known to cause pitting [Szklarska-Smialowska, 1971] and crevice corrosion [Davis & Streicher, 1985] [Oldfield & Sutton, 1978] as well. As shown in Figure 2-1 and Figure 2-2, HWC lowers crack acceleration arising from chlorides. It is important to note that no stress corrosion cracking, even with chlorides up to 10,000 ppm, have been observed if the dissolved oxygen level is less than 1 ppb [Gordon, 1980].

Typical sources of chloride in the BWR are from condenser tube leaks, from chloride containing organic solvents, and from organo-halides present in the water.

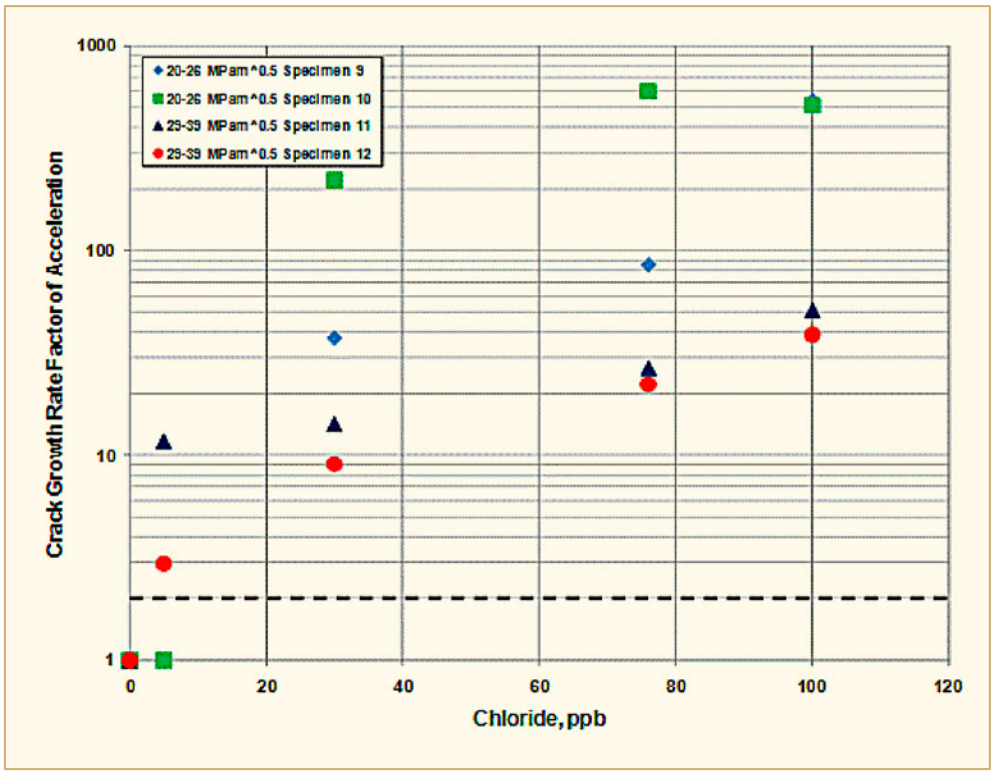

Figure 2-1: Crack growth rate acceleration of furnace sensitized Type 304 stainless steel as a function of chloride concentration in NWC [Gordon & Garcia, 2010].

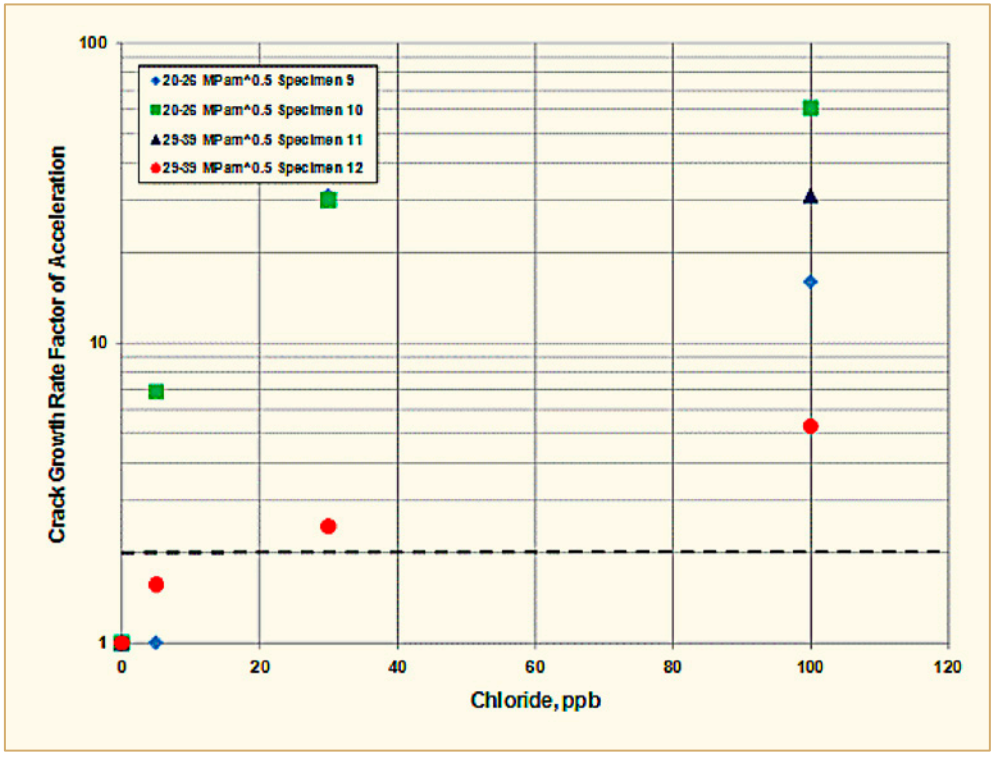

Figure 2-2: Crack growth rate acceleration of furnace sensitized Type 304 stainless steel as a function of chloride concentration in HWC [Gordon & Garcia, 2010].

2.1.2 Importance of minimizing sulphates

Sulphate contamination is also very detrimental to environmentally-assisted cracking (EAC) of materials in the BWR environment [Andresen, 1999], [Ruther & Kassner, 1983], [Andresen, 1983], [Indig et al, 1983], [Kurtz et al, 1983], [Shack, 1985], [Shack, 1986], [Ruther et al, 1988]. Figure 2-3 illustrates the accelerating effect of sulphate relative to the initiation of IGSCC as determined by SSRT [Gordon & Garcia 2010]. For example, the presence of approximately 1000 ppb of sulphate (>5 µS/cm conductivity due to sulphate) reduces the time for initiation of IGSCC by a factor of three over that experienced at 1 ppb sulphate in the NWC environment. (The vertical markers on the abscissa indicate the equivalent conductivities of sulphuric acid and sodium sulphate solutions).

As was the case with chloride, reversing DCPD crack growth rate studies with sulphate have also been performed on Type 304 stainless steel [König et al, 2004]. The detrimental effects of sulphate on furnace sensitized Type 304 stainless steel are shown in Figure 2-4 and Figure 2-5 for simulated NWC and HWC environments, respectively [Gordon & Garcia, 2010]. These crack growth rate factors of acceleration are also significantly greater than those identified for crack initiation, Figure 2-3.

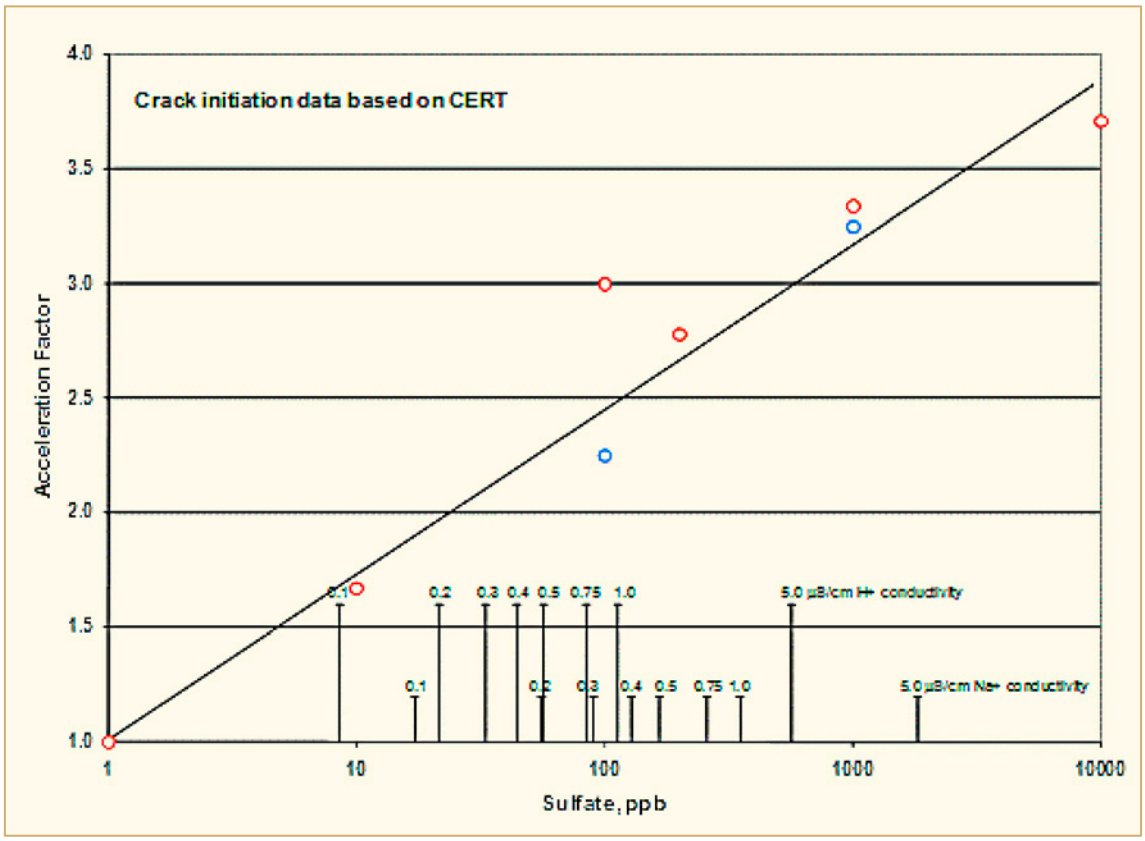

Figure 2-3: SCC initiation acceleration of furnace sensitized Type 304 stainless steel as a function of sulphate ion concentration added as sulphuric acid and sodium sulphate in 200 ppb dissolved oxygen at 288°C [Gordon & Garcia, 2010].

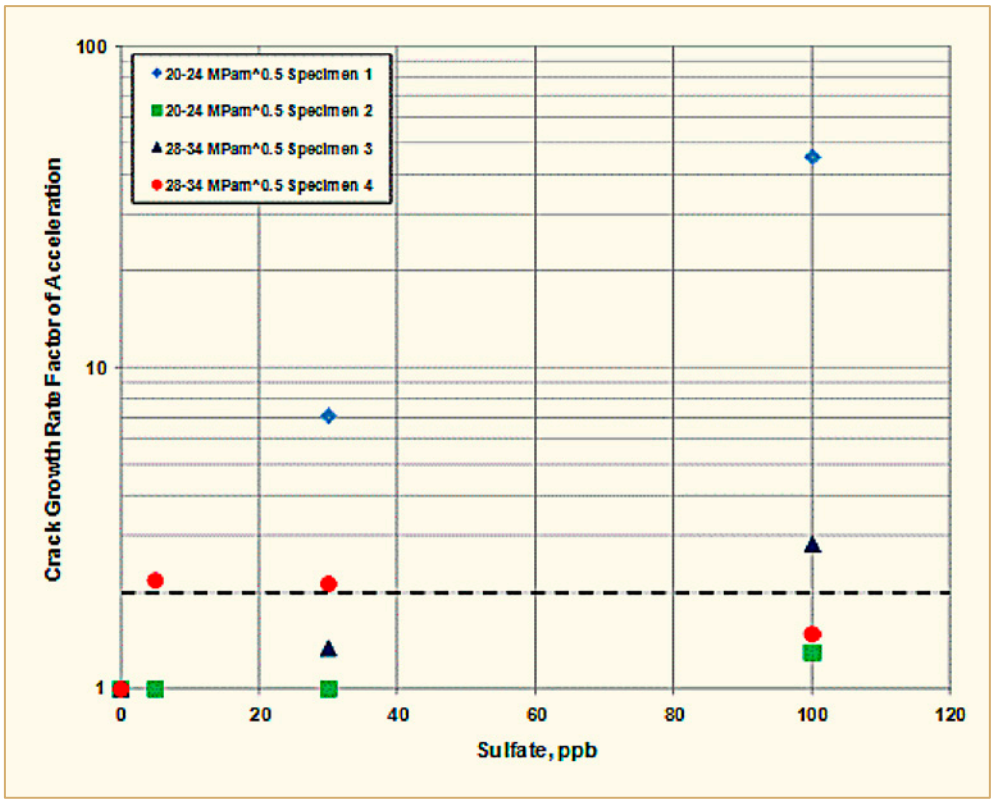

Figure 2-4: Crack growth rate acceleration of furnace sensitized Type 304 stainless as a function of sulphate concentration in NWC [Gordon & Garcia, 2010].

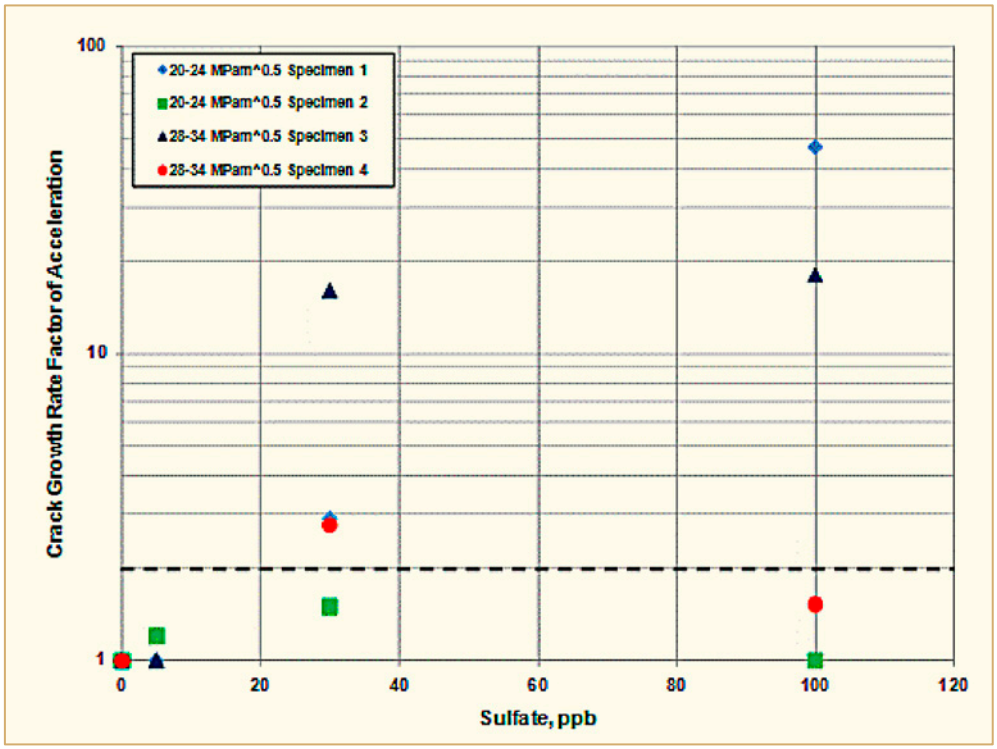

Figure 2-5: Crack growth rate acceleration of furnace sensitized Type 304 stainless as a function of sulphate concentration in HWC [Gordon & Garcia, 2010].

2.1.3 BWR water chemistry guidelines for chlorides and sulphates

A brief summary of BWR Water Chemistry Guidelines recommendations for reactor water chemistry specifically for chloride and sulphate control at power operating conditions are presented in Table 2-1 for NWC and HWC and HWC+NMCA operation [Garcia et al, 2010b].

Table 2-1: Summary of action levels of reactor water chlorides and sulphates, after [Garcia et al, 2010b].

Basis	Parameter	NWC	HWC or NMCA + HWC	Comments
Action Level 1	Sulphate and chloride	>5 ppb	>5 ppb	
Action Level 2	Sulphate and chloride	>20 ppb	>50 ppb	Credit for lower IGSCC rate under reducing chemistry regimes
Action Level 3	Sulphate and chloride	>100 ppb	>200 ppb	Credit for lower IGSCC rate under reducing chemistry regimes
Good Practice	Sulphate	<2 ppb	<2 ppb	Achievable based on plant experience
Good Practice	Chloride	<1 ppb	<1 ppb	Achievable based on plant experience
ANT International, 2012				

Different action levels are "briefly summarized" below, and more details of the action levels are presented in Section 3 of the LCC7 report Volume 1, [Cowan et al, 2011b].

Action Level 1 Value: This is the value of a parameter that, if exceeded, may threaten long-term system reliability, as indicated by data or engineering judgment, thereby warranting an improvement of operating practices. Corrective action is required within 96 hours. If not restored within 96 hours, a review needs to be performed to assess the impact on long-term system reliability, and management approval of a written plan and schedule to implement appropriate corrective actions is required [Gordon & Garcia, 2011], [Cowan et al, 2011b].

The Action Level 2 Value: Exceeding this action level indicates that significant degradation of the system may occur in the short-term. The first recommended response to a parameter exceeding an Action Level 2 value is to take corrective actions to reduce the parameter below the Action Level 2 values as soon as practicable. If the parameter has not been reduced below the Action Level 2 value within 24 hours at plants operating with NWC, or with HWC or NMCA+HWC during start-up, an orderly unit shutdown shall be initiated and the plant shall be brought to cold shutdown as rapidly as operating conditions permit.

At BWRs operating on HWC or HWC+NMCA, it may be more prudent to continue power operation with the HWC system in service during an excursion above Action Level 2 if this results in minimized degradation of components during the period of elevated impurity concentrations. An evaluation of probable impurity ingress scenarios shall be performed prior to occurrence of the event to document how continued operation rather than a shutdown will result in acceptable degradation of reactor materials if such an approach is adopted [Gordon & Garcia, 2011], [Cowan et al, 2011b].

3 Shutdown dose rate minimization (Robert Cowan)

3.1 Technical basics

3.1.1 Background

In the 1970s and early 1980s, General Electric and EPRI focused on identifying the sources of BWR shutdown doses as well as the mechanism by which the dose sources were established. This effort was called the BWR Radiation Assessment and Control (BRAC) program and provided the starting point for understanding how to minimize the resulting radiation fields [Anstine, 1977], [Romero, 1978], [Lin et al, 1980], and [Anstine, 1983].

The major findings of the BRAC program were:

- The majority of the dose (80-90%) in the drywell is due to the ^{60}Co isotope. Other contributors can be ^{58}Co, ^{54}Mn, ^{65}Zn, ^{59}Fe and ^{51}Cr.
- The majority (80-95%) of the ^{60}Co is incorporated into the corrosion film of the stainless steel piping in the drywell while the other 5-20% is associated with particles on the surface of the oxide film. See Table 3-1.
- The amount of Co and ^{60}Co in the corrosion film is proportional to the ***soluble*** concentration of Co and ^{60}Co in the reactor water.
- Feed water iron plays an important role in the generation and transport of ^{60}Co.
- "Hot spots" occur in low or disrupted flow areas and the dose in these areas is primarily due to particulate crud deposited from the water.
- Significant fuel failures can cause "spikes" in shutdown dose due to Zr-95 and Ru-103.
- For the short term, the only effective method for dealing with unacceptably high drywell dose rates is a recirculation piping system decontamination.

Table 3-1: Comparison of Fe, Ni, Cr, and ^{60}Co content in recirculation piping oxide films, after [Anstine, 1977].

Plant	Fe (mg/dm^2) (%)[a]	Ni (mg/dm^2) (%)[a]	Cr (mg/dm^2) (%)[a]	Co (mg/dm^2) (%)[ab]	^{60}Co (µ-Ci/cm^2) (%)[b]
BWR #9					
Outer layer	48 (95)	1.3 (3)	1.1 (2)	0.05 (17)	1.4 (12)
Inner layer	39 (80)	8.3 (16)	1.6 (3)	0.25 (83)	9.9 (88)
BWR #16					
Outer layer	11 (92)	0.6 (5)	0.6 (5)	0.03 (9)	0.4 (9)
Inner layer	61 (85)	8.1 (11)	3.8 (5)	0.31 (91)	3.8 (91)
BWR #11					
Outer layer	NA	NA	NA	NA	0.25 (7)
Inner layer	NA	NA	NA	NA	3.33 (93)
BWR #13					
Outer layer	NA	NA	NA	NA	0.39 (15)
Inner layer	NA	NA	NA	NA	2.05 (85)

[a] Percent of oxide layer.
[b] Percent distribution between layers.

ANT International, 2012

Since the time of the BRAC program there have been significant advancements in the understanding of how shutdown dose rates are established and how they can be controlled. This section will review both the phenomena involved in establishing shut down dose rates and the various methods used to minimize shut down dose rates in BWRs.

3.1.2 Radioactive species production and transport

The overall process of corrosion product transport, radioactive species production and out-of-core deposition is shown schematically in Figure 3-1. The overall transport processes are summarized below.

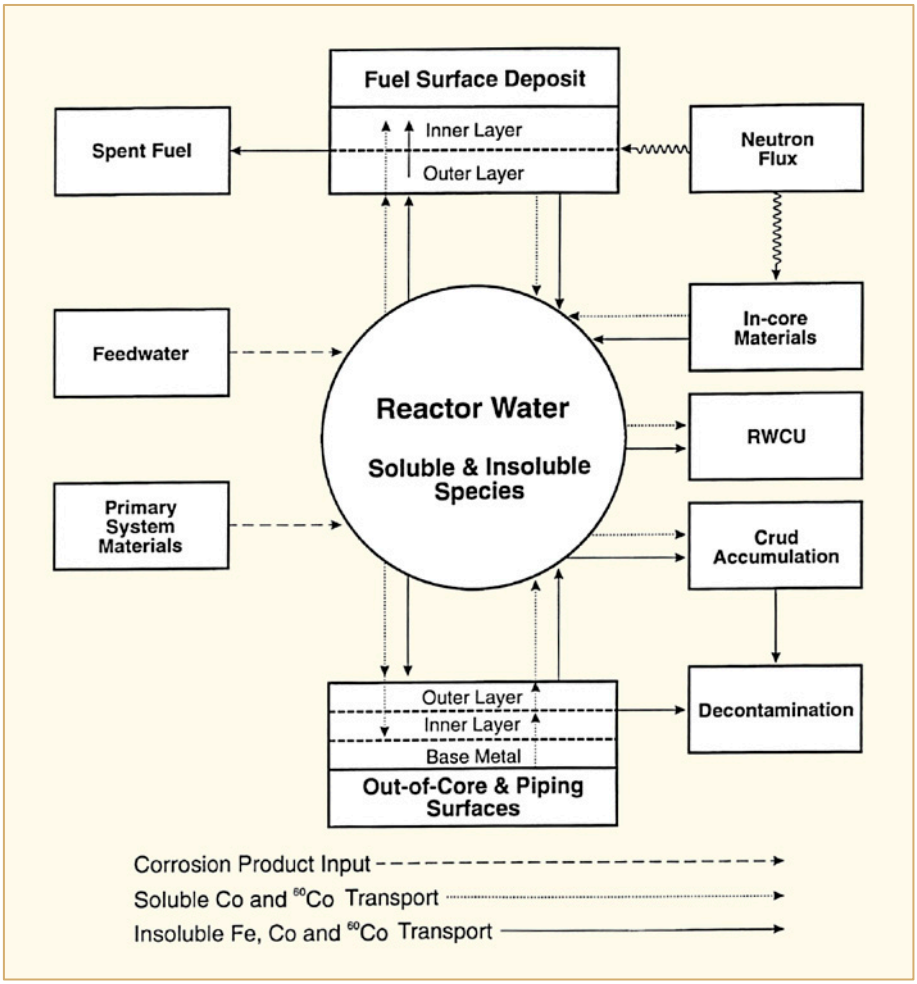

Figure 3-1: Schematic diagram of iron, Co and ^{60}Co production and transport [Lin, 1993].

1) The majority of the corrosion products[1] enter the reactor via the feed water, dominated in mass by Fe; however, other species such as Ni, Zn, Cu, Co, Mn, and Cr are also present. Colloids and particles of oxides and/or hydroxides are formed when their saturation limits are reached. The source of these species is the corrosion products released from the condensate and feed water systems that are not removed by the condensate treatment system. Forward pumped heater drains are also an important source of Fe input in plants so equipped. Metal ions and oxides are also released to the coolant from corrosion of the primary system components and piping.

2) Because iron, the most abundant species, is insoluble in high temperature pure water, it forms hydrated colloidal particles in the reactor water which serve as a surface for adsorption of ionic metallic species, such as Co, Ni, Zn, etc.

3) Both colloidal crud particles and soluble species deposit on the fuel heat transfer surfaces, but by different mechanisms. The neutron flux in the core activates the various components, resulting in the production of the isotopes shown in Table 3-2. Note that ^{60}Co has the longest half life and is gamma energy is very energetic and will be the focus of this discussion.

4) The radioactive species are released from the fuel surface deposits by any number of proposed mechanisms including: erosion, dissolution, hydraulic shear forces, ion exchange and particle spalling.

5) Radioactive species are released from the fuel deposits and activated core internals (such as control blades and fuel hardware) and removed by the reactor water cleanup system and out of core deposition, establishing a steady state concentration. The radioactive species are found in both "soluble" and "insoluble" forms, depending on their solubility and the presence of crud particles which act as scavengers. Soluble and insoluble radioactive species[2] are deposited on out-of-core surfaces by different mechanisms.

6) Soluble metallic cation species, such as ^{60}Co(s) are slowly incorporated into the oxide films of stainless steel components such as piping and serve as the main source of drywell radiation in most plants

7) Insoluble particles can deposit on out-of-core locations by several mechanisms and are often the major source of radiation fields in the pedestal room and control rod drive housings. Release of fuel crud particles containing ^{60}Co during shutdown/outages can provide doses in balance of plant and refuel locations.

In terms of total ^{60}Co inventory, over 99% remains locked in the fuel deposits and less than 1% is deposited in out of core locations. Unfortunately, because of the high absolute inventory of ^{60}Co, the 1% in out of core locations can cause significant operational issues and exposures. Logic diagrams such as that shown in Figure 3-1 serve as the basis for computer models that make calculations on a plant specific basis that predict reactor water ^{60}Co concentrations and shutdown dose rates [Lin & Garcia, 1994], [Lundgren et al, 1998] and [Kélen et al, 2004]. These models have proven to be effective under NWC conditions, but not as accurate with under HWC/Zn chemistries.[3]

[1] It is customary to refer to the corrosion product oxides by their elemental designation, not by their chemical form. Thus, Fe represents Fe^{+2}, Fe^{+3}, Fe_2O_3 and Fe_3O_4 and their hydrated forms. When the chemical form is important to understanding, it is stated.
[2] Insoluble species are defined as those that are collected by a 0.45 μm filter and soluble species are those collected on anion and cation filters immediately downstream of the 0.45 μm filter.
[3] See Section 2 for a detailed discussion of NWC and HWC water chemistry.

Table 3-2: Major activated corrosion products generated in the BWR [Cowan et al, 2011b].

Nuclide	Half life	Gamma energy (%ABN)	Formation reaction
Co-60	5.27 Yrs	1173 KeV (100%) 1332 KeV (100%)	Ni^{60} (n,p) Co^{60} Co^{59} (n,γ) Co^{60}
Mn-54	312 Days	834 KeV (100%)	Fe^{54} (n,p) Mn^{54}
Co-58	71 Days	811 KeV (99%) 511 KeV (30%)	Ni^{58} (n,p) Co^{58}
Fe-59	45 Days	1099 KeV (56%) 1292 KeV (43%)	Fe^{58} (n,γ) Fe^{59}
Cr-51	28 Days	320 KeV (9.8%)	Cr^{50} (n,γ) Cr^{51}
Zn-65	244 Days	1116 KeV (51%)	Zn^{64} (n,γ) Zn^{65}
Cu-64	12.7 Hrs	511 KeV (36%) 1346 KeV (0.5%)	Cu^{63} (n,γ) Cu^{64}
Fe-55	2.7 Yrs	No Gamma	Fe^{54} (n,γ) Fe^{55}
Mn-56	2.58 Hrs	847 KeV (99%) 1811 KeV (27%)	Mn^{55} (n,γ) Mn^{56}
Au-199	3.1 Days	Only β- at 452 KeV	Pt^{198}(n,γ)Pt^{199} Pt^{199}(β^-)Au^{199}
ANT International, 2011			

3.1.3 Incorporation of ^{60}Co into oxide films

When the BRAC program first hypothesized that ^{60}Co was somehow incorporating into the BWR piping corrosion films, a series of tests were conducted at GE to confirm this phenomenon. A loop was built to expose un-filmed stainless steel coupons to simulated BWR water chemistry over a range of soluble Co concentrations. The test conditions were high purity water maintained at simulated NWC conditions of 180 ppb O_2. The results, shown in Figure 3-2, showed that the Co/Fe ratio in the corrosion film is proportional to the soluble Co concentration over the range typical of that found in BWRs at the time. Note that 0.1 µg /l of Co in the water phase resulted in a 10^8 concentration factor of Co in the stainless steel oxide. A related result was reported in the BRAC program final report [Anstine, 1983] when reactor water soluble ^{60}Co was plotted vs. the BRAC dose rates[4] for newer plants. This plot was updated, Figure 3-3, utilizing data from both US and Japanese BWRs that were either new plants or had new recirculation system piping. Only plants operating with normal water chemistry (NWC), with or without Zn injection, were included. As will be discussed later, plants using one of the HWC methods mentioned in Section 2 combined with Zn injection do not show the direct proportionality of BRAC to ^{60}Co(s).

[4] The BRAC value is an average of the shielded dose rates measured on the vertical piping before and after the main recirculation pumps as described by [Palino, 1977].

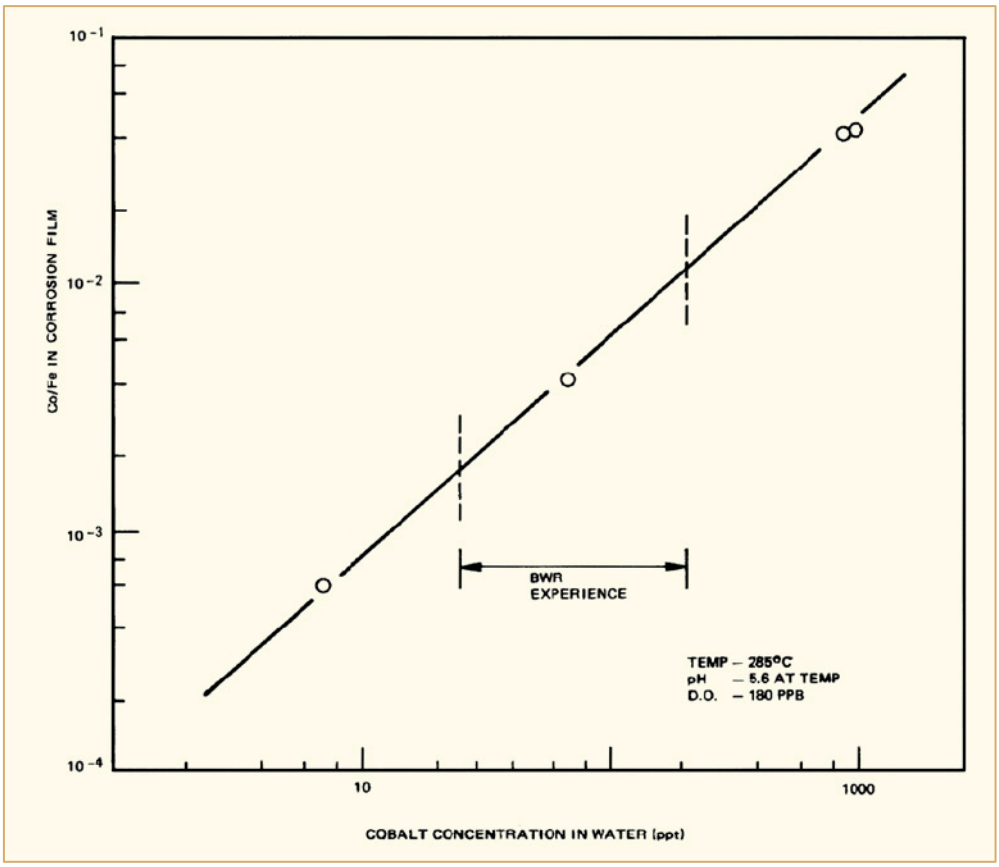

Figure 3-2: Incorporation ratio of cobalt in stainless steel corrosion film as a function of water cobalt concentration in pure, oxygenated water at 285°C [Niedrach, 1980].

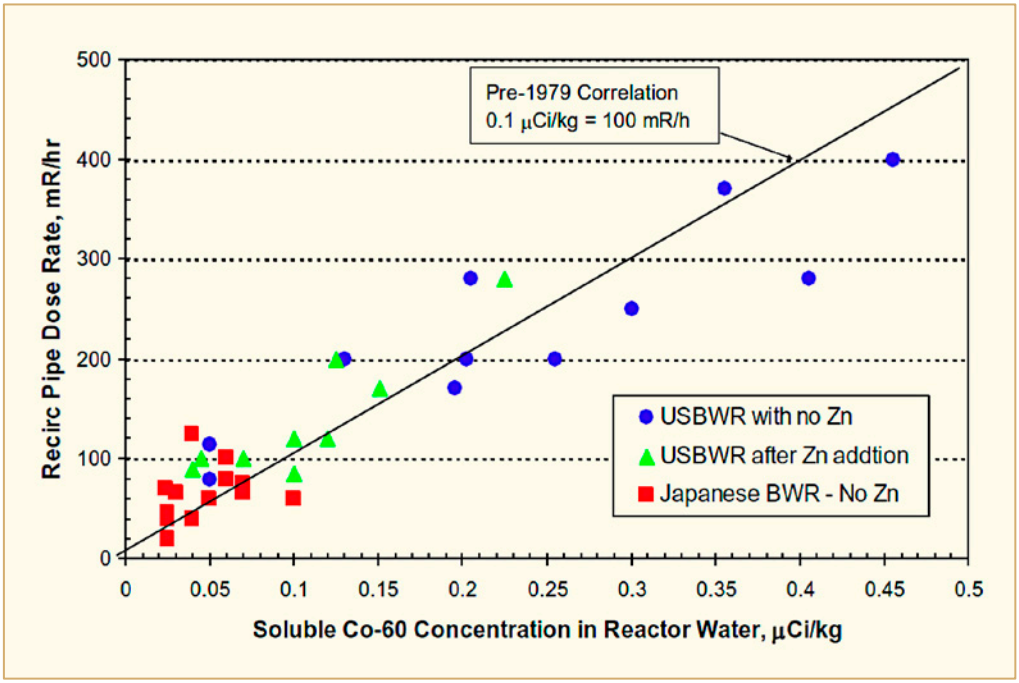

Figure 3-3: Correlation of recirculation piping dose rate with ^{60}Co(s) in reactor water under NWC conditions (pre-1985) [Lin, 1995].

4 Reactor water purity transients (Robert Cowan)

In Volume 1, Section 3 "Water chemistry guidelines and technical basis" we learned that there are recommended limits focussed on chronic impurity issues such as reactor water SO_4^{-2} and Cl^- levels. These guidelines from the Atomic Energy Society of Japan, EPRI and VGB also have recommendations on what to do if certain parameters are grossly exceeded, and as Table 4-1 shows, water purity transients can and do happen! The table shows the worse transients (in terms of reactor water conductivity) that have occurred according to [Gordon et al, 2012]. The EPRI Water Chemistry Guidelines-2008 Edition has a partial listing in an Appendix of the 86 such transients that have occurred during power operation and another listing of 33 transients that have occurred at shutdown. The major causes of these chemical transients are resin intrusions, condenser leaks and organic intrusions.[14]

Table 4-1: Top six water chemistry transients that have occurred during power operation ranked by peak conductivity value, after [Gordon et al, 2012].

Rank	Plant	Max Cond. µS/cm	pH	Max. Cl^- ppb	Max. SO_4^-, ppb	Water Chemistry	Date	Cause of Transient	Damange
1	Hamaoka 5	1194.0	8.5	379 000	67 000	NWC	05/17/11	Seawater injected into RPV due to Ti condenser failure	LPRM failures, TBD
2	DAEC	232.0	4.5	21 445	93 870	HWC + Zn + NMCA	02/01/03	SS condenser tube severed by baffle plate	Brief CGR increase
3	Fermi 2	182.0	10.6	12 000	10 000	NWC	12/25/93	Turbine blade through condenser, circ intrusion	2 LPRM failures, 16 SHB indications
4	Pilgrim	95.0	4.5	100		NWC	03/07/78	Condensate demineralizer resin bleed through	
5	Pilgrim	88.0				NWC	08/02/80	Condensate demin. resin intrusion	
6	Millstone	84.0	3.2	14 500		NWC	09/01/72	Condenser leak, demin. depleted	116/120 LPRM failures
ANT International, 2012									

When a significant water purity transient occurs, such as large increase in reactor water conductivity, SO_4^{-2} or Cl^- concentration, the VGB (and EPRI) recommend the following two alternatives:

- Initiate plant shutdown within 12 hours, or
- show that the plant chemistry can be returned to below the action level in less than the time to shut down to <100°C.

[14] The organics impurities are evidentially not noted by conductivity monitoring until they decompose in the reactor.

However, depending on the chemicals causing the purity transient, the conditions of time/temperature/chemistry that occur during a shutdown could be more damaging to reactor materials than remaining at temperature and pressure to correct the problem. This could be especially true for plants operating on moderate hydrogen water chemistry or using noble metal technology, where initiating a shutdown stops the input of feed water hydrogen and thus a drastic shift in ECP inside portions of the vessel that will aggravate the damage caused by both IGSCC and TGSCC processes.

As an example, Figure 4-1 from [Gordon et al, 2012] shows the crack growth rate behaviour of sensitized 304 stainless steel at 288°C in both NWC and HWC conditions under various conductivities due to SO_4^{-2} and Cl^- in the water. Since there is an order of magnitude increase in propagation rate in decreasing the hydrogen content (during a shutdown) it might cause less damage to remain at power if the cause of the transient were known and the time to reach benign reactor water chemistry conditions could be predicted.

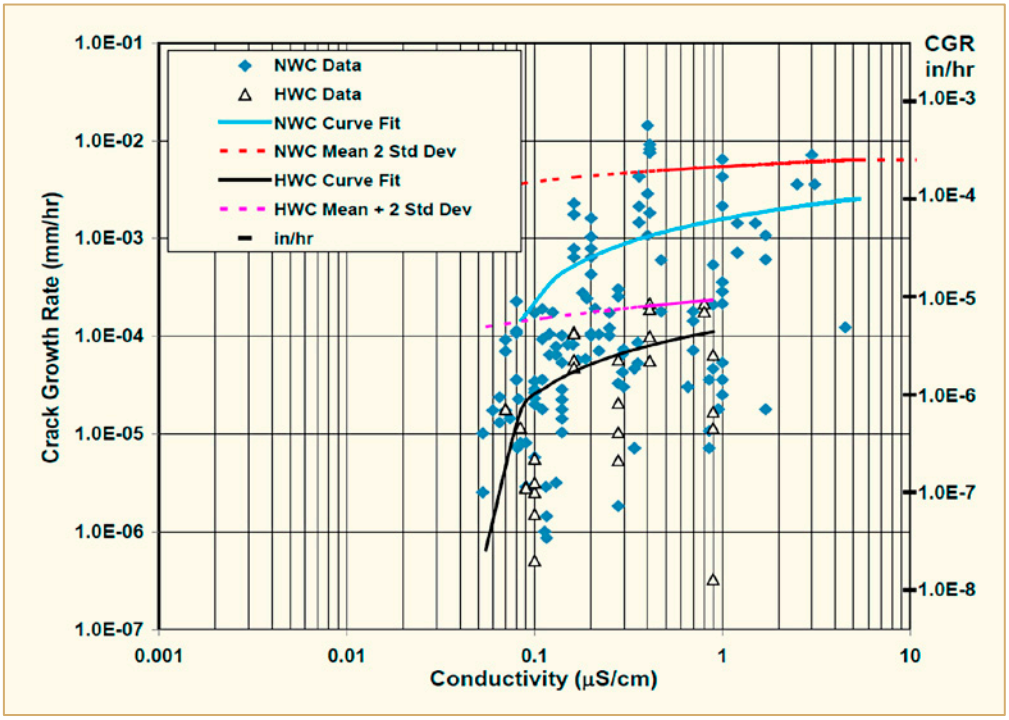

Figure 4-1: Comparison of NWC and HWC crack growth rate vs. conductivity for Type 304 stainless steel [Gordon et al, 2012].

Similarly, the effect of temperature on crack growth behaviour must be taken into account when making a decision regarding "stay hot or shut down" after a transient occurs. As shown in Figure 4-2 from [Garcia et al, 2010a], the crack growth under NWC (red line) increases from a value from one to two orders of magnitude when going from 288°C to 250°C and lower.

Because of the above factors, the EPRI Guidelines allow a third option in addition to the two above when a "shutdown" Action Level is exceeded during a purity transient during power operation:

- If an *a priori* evaluation of the type of the event and its severity has been performed and continued operation has been shown to result in less materials degradation than would occur during a shutdown/start-up sequence, power operation can be continued. For HWC or NMCA+HWC plants, the HWC system should remain in service if the decision is made to continue power operation.

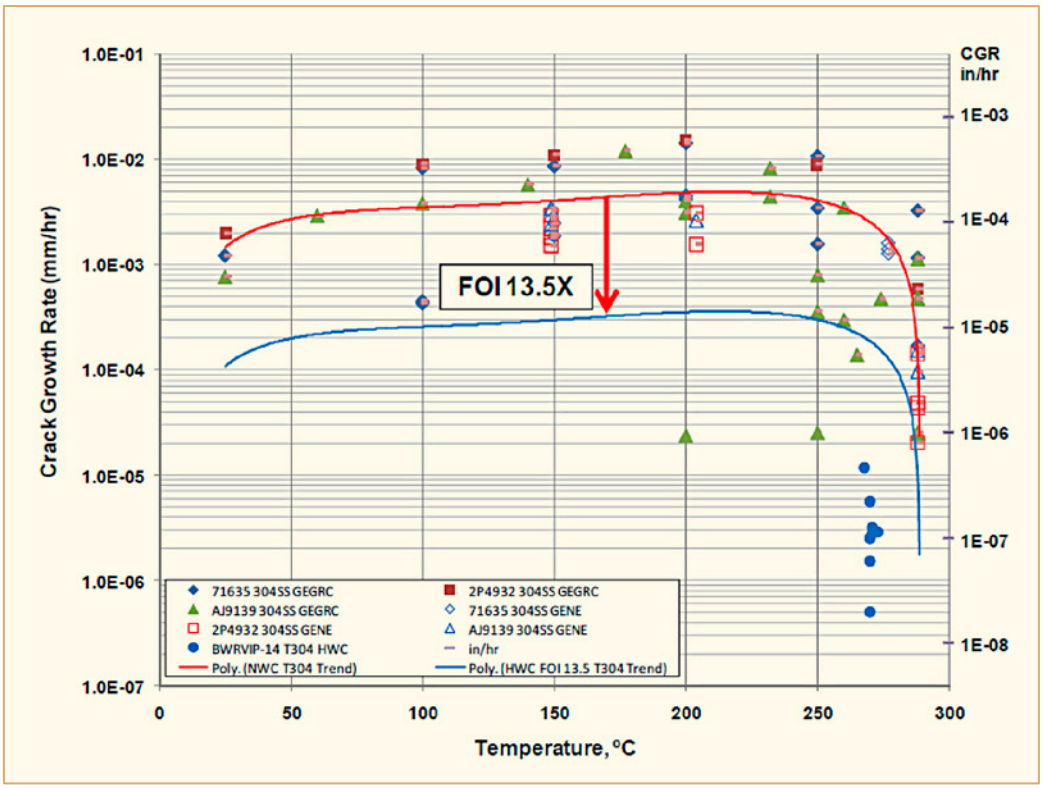

Figure 4-2: Effect of temperature on sensitized type 304 stainless steel and sensitized alloy 600 crack growth rates in 200 ppb oxygenated water and an estimate of the growth under HWC conditions if the factor of 13.5 times improvement at 288°C were true at intermediate temperatures [Garcia et al, 2010a].

The key phrase above is “a priori evaluation”. Using the available worldwide reports of purity intrusion events, each BWR owner should develop their own decision tree analysis for those cases that could be applicable to them. Such a decision tree is shown in Figure 4-3 for the case of a condenser tube leak. Each decision tree should be supported with an engineering analysis showing the expected crack growth under the expected scenarios considered. If similar purity transient were to happen at the station, the “a priori evaluation” would be available and the prudent path to deal with the issue would be available.

5 Surveillance Programs (Wilfried Rühle)

5.1 NWC plants

The following remarks about the surveillance programs are limited to the reactor water cooling system and the balance of the plant with the connected auxiliary systems. Because of the water chemistry in NWC- plants using ultra pure demineralised water only without any addition of chemicals, besides the gases hydrogen and oxygen from water radiolysis, the basic chemical surveillance can be done by measurements of conductivity and, when indicated, oxygen concentration. Both can be made by continuously working on-line instrumentation. Even introduced organics, especially from ion exchanger release, can be detected by conductivity measurements, as they are cracked in the radiation field and oxidized there to CO_2. Figure 5-1 shows the recommended locations for the on-line instrumentation at the examples of a cascaded (left part) and a forward pumped BWR.

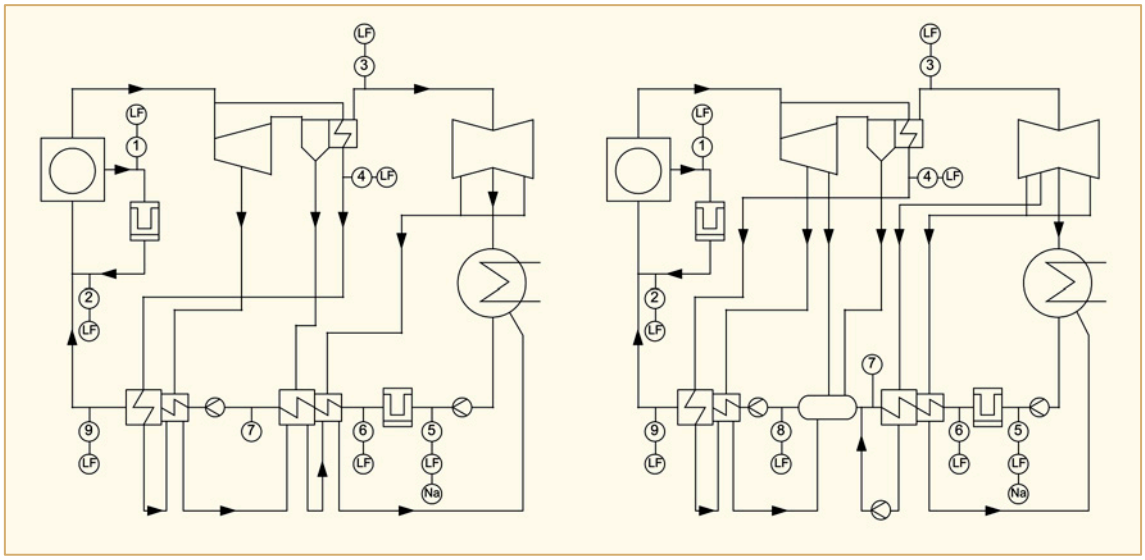

Figure 5-1: Recommended locations for on-line conductivity measurements in BWRs with cascaded (left part) and forward pumped condensates (LF = conductivity) [Odar et al, 2010].

The surveillance locations are reactor water upstream reactor water clean-up system (1), reactor water downstream reactor water clean-up system (2), main steam downstream reheater (3), reheater condensate (4), main condensate upstream condensate purification system (5), main condensate downstream condensate purification system (6), condensate downstream low pressure pre-heaters (7), feed water downstream feed water tank (only in right part) (8), and final feed water (9).

The continuously working oxygen measurements should be made in the condensate downstream the condenser to check the efficiency of the condensate degasification, upstream and downstream the feed water tank (if installed) to check the efficiency of feed water degasification, and upstream the reactor or respectively downstream the high pressure pre-heaters, to check if there is enough oxygen in feed water to protect the high pressure pre-heaters.

Very important is the continuous surveillance of the condenser integrity. This can be realized by using a system for continuous conductivity and sodium measurement in each compartment of the condenser (Figure 5-2). Operational experience has shown that conductivity measurement alone doesn't give unequivocal information about leakages (Figure 5-3), but Na- measurement does.

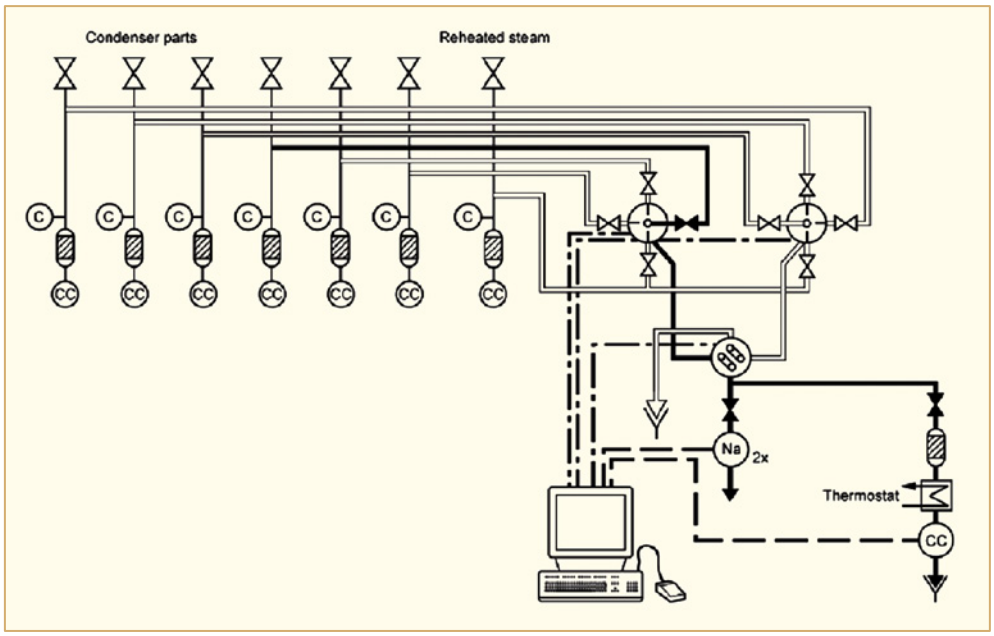

Figure 5-2: Equipment for continuous conductivity and sodium measurement in each compartment of the condenser [Böttcher & Rühle, 2007].

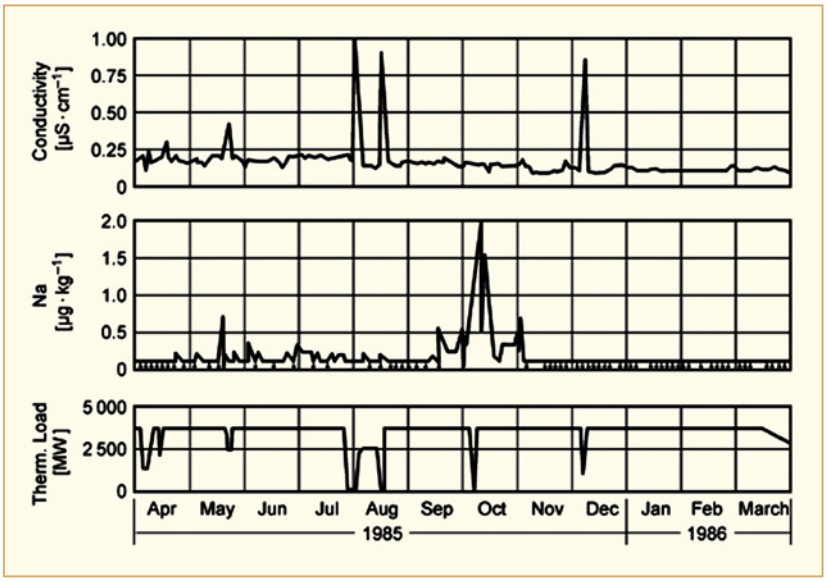

Figure 5-3: Operational experience showing that only both, conductivity measurement and Na- measurement, give reliable information about condenser leakages [Böttcher & Rühle, 2007].

Continuous surveillance of conductivity and oxygen is a very important contribution to save and economic plant operation. Additionally, to ensure save and economic operation for the lifetime of the plant and to prove compliance with the national guidelines and the technical specifications of the plant, other measurements by grab-samples are essential. The reasons are detection of potential corrosion problems in the reactor and the balance of the plant and acquiring data for counteractive measures, surveillance and control of activity build-up, and ensuring good fuel performance by avoiding coolant related corrosion. Another important task is measurement of fission products for detection of kind and number of fuel leakages. Table 5-1, Table 5-2, Table 5-3 and Table 5-4 summarize the parameters, which are recommended to be measured, and the related measurement frequencies, depending on the operational status of the plant.

5.1.1 Reactor water

The measurements of impurities in the reactor water are very effective, as especially corrosive ions are concentrated in the water due to water evaporation by a factor of up to 100, depending on the purification rate of the clean up systems. Thus, traces of impurities can be measured easily. In case of suspended solids, there is a contest between deposition, concentration, reduction by the purification system, and, not to forget, volatility with steam. Sampling and measurement of solids needs experienced and skilled personnel.

Table 5-1: Recommended surveillance program for reactor water in BWRs with NWC.

		Reactor water during operation (upstream and downstream of the purification system)	**Reactor water during cold shut down and preparedness for start up (<100°C)**	**Reactor water during preparedness for start up**	**Reactor water during start up until normal operation**	**Reactor water during shut down**
Parameter	Control or diagnostic	Frequency of measurement	Frequency of measurement	Frequency of measurement	Frequency of measurement	Frequency of measurement
Conductivity (25°C)	Control parameter	Continuously	Three times a week or continuously for start up preparedness	Continuously	Continuously	Continuously
Chloride	Control parameter	Once a week	Three times a week	Once a day or more during preparedness for start up	Once a day	
Sulphate	Control parameter	Once a week	Three times a week		Once a day	
pH (25°C)			If cond. >2μS/cm			
Silica	Diagnostic parameter	Once a week			Once a day	
Iron $_{total}$	Diagnostic parameter	Once a week				On demand for determination of crud behaviour
Copper $_{total}$	Diagnostic parameter	Once a week				On demand for determination of crud behaviour
Suspended solids	Diagnostic parameter	In case of special reasons				On demand for determination of crud behaviour
γ –gross-activity	Diagnostic parameter	Three times a week	Three times a week		Once a day	Every two hours
Nucl. spec. γ-activity	Diagnostic parameter	Three times a week	Once a week		Once a day	Every two hours
Iodine- nuclides	Diagnostic parameter	Three times a week	Once a week		Once a day	Every two hours
Other radionuclides (Cs, Np, etc.)	Diagnostic parameter	Once a week or for special reasons				

ANT International, 2012

6 References

Abe A, Tobita H., Nagata N., Dozaki K. and Takiguchi H., Nuclear Sci. and Eng. 149, 312, 2005.

Adamson R., Garzarolli F., Cox B., Strasser A. and Rudling R., *Corrosion Mechanisms in Zirconium Alloys*, ZIRAT12, Special Topic Report, 2007.

Alder H. P. and Brélaz P., *Overview of activities for the reduction of dose rates in Swiss boiling water reactors*, Water chemistry in nuclear Reactor Systems 6, BNES, London, 1992.

Andresen P. L., EPRI Report NP-3384, Palo Alto, CA, November, 1983.

Andresen P. L. and Ford F.P., Materials Science & Engineering, A 103, pp167-184, 1988.

Andresen P. L. and Angeliu T., CORROSION/96, Paper #84, T-2A Symposium, NACE, March, 1996.

Andresen P. L., 9th International Symposium on Environmental Degradation of Materials in Nuclear Power Systems - Water Reactors, Newport Beach, CA, page 411, August 1-5, 1999.

Andresen P. L., Catlin W. R. and Emigh P.W., Paper # 03666, CORROSION/2003.

Andresen P. L, Diaz T. P. and Hettiarachchi S., Paper# 04668, CORROSION/2004.

Andresen P. L., 13th Int Symp. on Env. Degradation of Materials in Nuclear Power Systems-Water Reactors, NACE International, August, Vancouver, Canada, 2007.

Andresen P. L., Kim Y. J., Diaz T.P. and Hettiarachchi S., CORROSION/2008, Paper#08601, T-2A Symposium, NACE, March, 2008.

Anstine L. D., *BWR Decontamination and Corrosion Product Characterization*, General Electric Report NEDE-12665, 1977.

Anstine L. D., *BWR Radiation Assessment and control Program: Assessment and control of BWR Radiation fields*, EPRI Report NP-3114, May 1983.

Asakura Y. et al., *Current Operating Experience With Water Chemistry In Crud Concentration Suppressed Boiling Water Reactors*, International Conference on Water Chemistry of Nuclear Reactor Systems -5, Bournemouth, UK, Oct. 23-27, 1989.

Baston V. F., Garbauskas M. F. and Oken H., *Material Characterization of films on BWR Components Exposed to Hydrogen Water Chemistry and Zinc Injection,* International Conference on Water Chemistry of Nuclear Reactor Systems -7, Bournemouth, UK, October 1996.

Beverskog B. and Puigomenech I., *Stability of Fuel Crud in BWR*, International Conference on Water Chemistry of Nuclear Reactor Systems -7, Bournemouth, UK, October 1996.

Bradbury D., *Review of Decontamination Technology Development 1977-2000*, International Conference on Water Chemistry of Nuclear Reactor Systems -8, Bournemouth, UK, October 2000.

Brunk J., *System decontamination of two BWR units performed during 2011 and 2012*, ISOE 2012, Prague, 2012.

Brunning P., Bengtsson B., Granath G. and Kvint J., *Corrosion Product Measurements at Ringhals 1*, International Conference on Water Chemistry of Nuclear Reactor Systems -7, Bournemouth, UK, October 1996.

Böttcher F. and Rühle W., *Mandatory and Desirable Instrumentation in PWR and BWR units*, Power Plant Chemistry 2007, 9(1).

BWRVIP-69, TR-112868, *Post-NMCA Fuel Surveillance Program at Duane Arnold*, June, 1999.

BWRVIP-130 - EPRI TR-1008192, *BWR Water Chemistry Guidelines – 2004 Revision*, Palo Alto, CA, October 2004.

BWRVIP-159, EPRI Technical Report 1013397, *BWR Vessel and Internals Project*, *HWC/NMCA Experience Report and NMCA Applications Guidelines*, Final Report, 2006.

BWRVIP-174, TR-1014994, *Review of BWR Core Shroud Inspection Results for Plants Mitigated with NMCA and HWC*, September, 2007.

BWRVIP 190, EPRI 1016579, *BWR Water Chemistry Guidelines*, Palo Alto, CA, 2008.

BWRVIP-258 - EPRI 1023222, *BWR Radiolysis and ECP Analysis*, Palo Alto, CA, 2011.

Callister W. D. (Univ. of Utah), *Materials Science and Engineering: An Introduction* 7th Edition with Wiley Plus Set, February, ISBN: 978-0-470- 11341, 2008.

Cheng B., Adamson R. B., Machiels A. J. and O'Boyle D., *Effect of Chemistry on Fuel Performance at Dresden-2*, Proceedings of International Topical Meeting on LWR Fuel Performance, Avignon, France, pp 664-681, April 21-24, 1991.

Cheng B., Turnage K. G., Potts G. A., Lutz D. R., Pathania R. S., Rohrer R. J., Eyre M. and Armstrong E., *Proceedings International Meeting on LWR Fuel Performance*, Orlando, Florida, September, 2004.

Cheng B., Smith F. and Lemons J., *BWR Fuel Reliability under Challenging Water Chemistry Conditions*, Paper 2149, Proceedings of Top Fuel 2009, Paris, France, September 6-10, 2009.

Chopra O. K., *Degradation of LWR Core Internal Materials due to Neutron Irradiation*, NUREG/CR- 7027, 2010.

Congleton J., Zheng W. and Hua H., Corrosion Science, Vol. 30, No. 6/7, page 555,1990.

Cowan R. L. et al, *Hydrogen Water chemistry Operating Experience*, Post-SMIRT Conference, Ispra, Italy, August 1985.

Cowan R. L., Lin C. C., Marble W. J. and Skarpelos, J. M., *Recent Developments in BWR Water Chemistry*, 2nd International Topical Meeting on Nuclear Power Plant Thermal Hydraulics and Operations, Tokyo, Japan, April 15-18, 1986.

Cowan R. L., Lin C. C., Marble W. J. and Ruiz C. P., 5th International Symposium on Environmental Degradation of Materials in Nuclear Power Systems-Water Reactors, Monterey, CA, August 25-29, 1991.

Cowan R. L. and Marble W. J., *Hydrogen Water Chemistry Effects on BWR Radiation Buildup - Preliminary Evaluation of Plant Data*, EPRI TR-101463, November, 1992.

Cowan R. L. and Kiss E., 6th International Symposium on Environmental Degradation of Materials in Nuclear Plants, San Diego, Calif., August 1993.

Cowan R. L., Proceedings of VGB Conference on Power Plant Chemistry, Essen, Germany, October 1994.

Cowan R. L., 7th International Conference on Water Chemistry of Nuclear Reactor Systems, Bournemouth, UK, October 1996.

Cowan R. L. and Garcia S. E., *Zinc Addition Experience in BWRs Under Normal and Hydrogen Addition Chemistry,* International Conference on Water Chemistry in Nuclear Power Plants, Kashiwazaki, Japan, Oct. 13-16, 1998.

Cowan R. L, Hettiarachchi S., Hale D. A. and Law R. J., Proc. Water Chemistrty'98, JAIF, p.419, Oct 13-16, Kashiwazaki, Japan, 1998a.

Cowan R. L., Adamson R. B., Garcia S. E., Potts G. A., Levin H. A. and Armijo J. S., *BWR Water Chemistry Strategies for Simultaneously Minimizing Fuel Clad Corrosion, Mitigating IGSCC, and Minimizing Shut Down Dose Rates,* European Nuclear Conference, Nice, October, 1998b.

Cowan R. L. and Wood C. J., *Control of Radiation Fields in BWRs After Noble Metal Chemical Addition*, Water Chemistry in Nuclear Reactor Systems, CHIMIE 2002, April 22-26, Avignon, France, 2002.

Cowan R. L., *Cofrentes Dose Rate Root Cause Study,* BWRVIP Mitigation Meeting, Santa Fe, New Mexico 2005.

Cowan R. L. and Hussey D., *Radiation Field Trends as Related to Chemistry in United States BWRs*, 2006 International Conference on Water Chemistry of Nuclear Reactor Systems - Jeju Island, Korea, Oct 23-26, 2006.

Cowan R. L., from personal files, 2010.

Cowan R. L. and Garcia S. E., *The Technical Basis For Limiting Copper In The BWR Primary Coolant*, Nuclear Plant Chemistry Conference 2010, Quebec City, Canada, October 3-7, 2010.

Cowan R. L., Varela J. and Garcia S.E., *The Effect Of On-Line Noble Metal Addition On The Shut Down Dose Rates Of Boiling Water Reactors*, 15th Environmental Degradation Conference, Colorado Springs, Colorado Springs, Colorado, August 2011a.

Cowan R. L., Rühle W. and Hettiarachchi S., *Introduction to Boiling Water Reactor Chemistry – Volume 1*, LCC7 Special Topic Report, ANT International, Mölnlycke, Sweden, 2011b.

Cowan R.L. and Garcia S.E., *The Role of Noble Metal Addition Methods on BWR Shut Down Dose Rates*, Nuclear Plant Chemistry Conference 2012, Paris, Sept. 24-28, 2012.

Cowan R. L., Garcia S. E. and Goldstein J., *BWR Chemistry Impacts on Shut Down Dose Rates*, International Boiling Water Reactor and Pressurized Water Reactor Materials Reliability Program Conference and Exhibition 2012, Washington D.C., National Harbor, Maryland, National Harbor, Maryland, July 16-19, 2012.

Davis G. O. and Streicher M. A., Corrosion/85, NACE, Boston, MA, March 25, 1985.

Duncan F., *Rickover: The Struggle for Excellence, Naval Institute* Press (2001), ISBN 1-55750-177-7 (alk. paper), 2001.

Duncan R., *Recontamination Mitigation by Passivation*, EPRI Radiation Reduction Workshop, Palo Alto, CA, 2011.

Eickelpasch N. and Lasch M., *Investigations on Transport and Activation of Corrosion Products in the 2X1300 MW_{el} Boiling water Reactors of Gundremmingen*, International Conference on Water Chemistry of Nuclear Reactor Systems -4, BNES, London, UK, October, 1987.

EPRI Report TR-103296, *Cobalt Reduction Guidelines*, Rev. 1, Palo Alto, CA, 1993.

EPRI Report TR-101463, *Hydrogen Water Chemistry Effect on BWR Radiation Buildup*, Volumes 1 through 5, November, 1995.

EPRI Report 1016579, *BWR Water Chemistry Guidelines*, BWRVIP-190: BWR Vessel and Internals Project, October, 2008.

EPRI Report 1019072, *BWR Vessel and Internals Project, BWR Shutdown and Startup Chemistry Experience and Application Sourcebook*, BWRVIP-225, Palo Alto, CA, 2009.

EPRI Report 1021103, *Cobalt Reduction Sourcebook*, Palo Alto, CA, 2010.

EPRI Report 1025319, *Boiling Water Reactor Shutdown Chemistry and Dose Summary: 2012 Update*, Palo Alto, CA, 2012.

Erve M., Leitz C. and Roth A., *Alterung von Strukturwerkstoffen im Kernbereich des RDB,* SVA Vertiefungskurs, Winterthur, Schweizerische Vereinigung für Atomenergie, 2. Bis 4. Nov. 1994.

Falk C. F., *BWR Cobalt Source Identification*, EPRI-NP-2263, Palo Alto, CA, 1982.

Fejes P., Seminar on Counter Measures for BWR Pipe Cracking, Electric Power Research Institute, Palo Alto, California, January, 1980.

Flores C. D., *Evaluation of Radiation Induced Segregation in Fe-Ni.Cr Alloys*, Master Thesis, Massachusetts Institute of Technology, Mai 1994.

Forsberg S., Odelius H., and Granath G., *Release Rates from Stellite in Simulated Boiling Water Reactor Environments*, Water Chemistry of Nuclear Reactor Systems, San Francisco, Oct. 2004.

Frattini, P. L. et al., *Sequestration Resins for Accelerating Removal of Radioactive Contaminants*, IEX 2012: The International Ion Exchange Conference, Cambridge, UK, Sept. 19-21, 2012.

Garcia S. E. and Cowan R. L., *Zinc Addition Experience in BWRs Under Normal and Hydrogen Addition Chemistry* Japan International Conference on Water Chemistry in Nuclear Power Plants, Water Chemistry 98, Kashiwazaki, Japan, October 13-16, 1998.

Garcia S. E., Tran P., Gianelli J. F., Jarvis A. J. and Jarvis M. L., *BWR Source Term Management – Strategies And Results At General Electric-Designed BWRs*, I.S.O.E. International Symposium Poster Session, Cambridge, UK, Nov. 17-19, 2010a.

Garcia S. E., Giannelli J. and Jarvis M., Nuclear Plant Chemistry Conference 2010, Quebec City Canada, October 3-7, 2010b.

Garcia S. E., Tran P., Gianelli J. F. and Jarvis M. L., *Advances in BWR Water Chemistry*, Nuclear Plant Chemistry Conference 2012, Paris, Sept. 2012a.

Garcia S. E., Odell A.D. and Gianelli J. F., *Early Hydrogen Water Chemistry Project Review, Improvement Opportunities And Conceptual Design Options At Exelon Boiling Water Reactors,* Nuclear Plant Chemistry Conference 2012, Paris, Sept. 2012b.

Gordon B. M., Materials Performance, Vol. 19, No. 4, page 29, April 1980.

Gordon B. M. and Garcia S. E., Nuclear Plant Chemistry Conference 2010, Quebec City Canada, October 3-7, 2010.

Gordon B. M., Garcia S.E. and Odell D., *BWR Chemistry Transients - Experience and Guidance*, International Boiling Water Reactor and Pressurized Water Reactor Materials Reliability Program Conference and Exhibition 2012, Washington D.C., National Harbor, Maryland, National Harbor, Maryland, July 16-19, 2012.

Hemmi Y., Ichikawa N., Saito N., Morikawa Y. and Nagao H., *Passivation Mechanism of Oxide Films Formed on Inconel X-750 in simulated BWR Core Environment*, Water Chemistry of Nuclear Systems 5, BNES, London, 1989.